Physics Letters B 758 (2016) 321–346

Contents lists available at ScienceDirect

Physics Letters B

www.elsevier.com/locate/physletb

Measurement of spin correlations in $t\bar{t}$ production using the matrix element method in the muon+jets final state in pp collisions at $\sqrt{s} = 8$ TeV

CMS Collaboration *

CERN, Switzerland

ARTICLE INFO

Article history:
Received 19 November 2015
Received in revised form 14 March 2016
Accepted 2 May 2016
Available online 6 May 2016
Editor: M. Doser

Keywords:
CMS
LHC
Top quark
Matrix element method
Spin

ABSTRACT

The consistency of the spin correlation strength in top quark pair production with the standard model (SM) prediction is tested in the muon+jets final state. The events are selected from pp collisions, collected by the CMS detector, at a centre-of-mass energy of 8 TeV, corresponding to an integrated luminosity of 19.7 fb^{-1}. The data are compared with the expectation for the spin correlation predicted by the SM and with the expectation of no correlation. Using a template fit method, the fraction of events that show SM spin correlations is measured to be $0.72 \pm 0.08\,(\text{stat})^{+0.15}_{-0.13}\,(\text{syst})$, representing the most precise measurement of this quantity in the muon+jets final state to date.

© 2016 The Author. Published by Elsevier B.V. This is an open access article under the CC BY license (http://creativecommons.org/licenses/by/4.0/). Funded by SCOAP[3].

1. Introduction

At the CERN LHC top quarks are predominantly produced in pairs ($t\bar{t}$), mainly via gluon fusion, with each top quark decaying almost 100% of the time into a W boson and a b quark. The final states can be categorised as dilepton, where both W's decay into a lepton and a neutrino, hadronic, where both W's decay into quarks, and lepton+jets otherwise. The W decay into a tau lepton and neutrino is only considered leptonic if the τ decays include a muon or electron.

In quantum chromodynamics (QCD), the quark spins in heavy quark production are correlated. Since the lifetime of top quarks is smaller than the hadronisation timescale ($1/\Lambda_{\text{QCD}}$), which in turn is smaller than the spin decorrelation timescale $m_t/\Lambda^2_{\text{QCD}} \sim 3 \times 10^{-21}$ s, the top quarks decay before their spins decorrelate. This spin correlation is therefore propagated to the top quark decay products and one can infer the $t\bar{t}$ spin correlation strength A by studying the angular correlations between the decay products, where

$$A = \frac{(N_{\uparrow\uparrow} + N_{\downarrow\downarrow}) - (N_{\uparrow\downarrow} + N_{\downarrow\uparrow})}{(N_{\uparrow\uparrow} + N_{\downarrow\downarrow}) + (N_{\uparrow\downarrow} + N_{\downarrow\uparrow})} \tag{1}$$

is the asymmetry between the number of $t\bar{t}$ pairs with aligned and antialigned spins. The value of A depends on the spin quantization axis chosen and on the production modes.

Given the high centre-of-mass energy at the LHC, the helicity basis is used where the spin quantization axis is defined as the top quark or antiquark direction in the $t\bar{t}$ rest frame. The corresponding value of the spin correlation strength in the helicity basis is referred to as A_{hel}. Since the spin correlation strength is precisely, but non-trivially, predicted by the standard model (SM) an accurate measurement of this variable tests various aspects of the SM, including the strength of the QCD coupling and the relative contribution of $t\bar{t}$ production modes, although new physics can influence the spin correlation strength [1,2].

Tevatron experiments made measurements of the $t\bar{t}$ spin correlation strength using template fits to the angular distributions of the top quark decay products and extracting the fraction of $t\bar{t}$ events with the SM prediction of spin correlation f defined as

$$f = \frac{N^{t\bar{t}}_{\text{SM}}}{N^{t\bar{t}}_{\text{SM}} + N^{t\bar{t}}_{\text{uncor}}}, \tag{2}$$

where $N^{t\bar{t}}_{\text{SM}}$ is the number of SM $t\bar{t}$ events, whereas $N^{t\bar{t}}_{\text{uncor}}$ represents the number of events with uncorrelated $t\bar{t}$. The top quark and antiquark in the uncorrelated $t\bar{t}$ events decay spherically. The assumption is that there are only SM and uncorrelated $t\bar{t}$ events,

* *E-mail address:* cms-publication-committee-chair@cern.ch.

http://dx.doi.org/10.1016/j.physletb.2016.05.005
0370-2693/© 2016 The Author. Published by Elsevier B.V. This is an open access article under the CC BY license (http://creativecommons.org/licenses/by/4.0/). Funded by SCOAP[3].

with a fraction of $(1-f)$ of uncorrelated $\mathrm{t\bar{t}}$ events. The physical range of this parameter f is restricted to [0, 1], with $f=1$ for a sample of $\mathrm{t\bar{t}}$ events produced by the SM. However, quite often an unconstrained template fit is performed, allowing for non-physical values of this parameter. The CDF Collaboration extracted the fraction f of events with the SM prediction of spin correlation using the lepton+jets final state [3] and the D0 Collaboration extracted this fraction using the dilepton final states [4,5]. The D0 Collaboration also made a spin correlation measurement using the matrix element method (MEM) [6] in the dilepton final state and found direct evidence of $\mathrm{t\bar{t}}$ spin correlation by combining the measurements using MEM in the dilepton and lepton+jets final states [7]. The combined measurement yielded $f = 0.85 \pm 0.29\,(\mathrm{stat} + \mathrm{syst})$ using a data sample of $\mathrm{p\bar{p}}$ collisions at $\sqrt{s} = 1.96\,\mathrm{TeV}$, corresponding to an integrated luminosity of $5.3\,\mathrm{fb}^{-1}$.

At the LHC, the ATLAS Collaboration has reported observation of spin correlations in top quark pair production [8]. In the most recent measurement by the ATLAS Collaboration, the spin correlation measurement was performed using template fits to the distribution of the difference in azimuthal angle between the two oppositely charged leptons in the dilepton final state. This measurement at $\sqrt{s} = 8\,\mathrm{TeV}$, using $20.3\,\mathrm{fb}^{-1}$ of integrated luminosity, resulted in $f = 1.20 \pm 0.05\,(\mathrm{stat}) \pm 0.13\,(\mathrm{syst})$ [9]. Another result by ATLAS in the dilepton channel has been reported in [10]. The only measurement in the lepton+jets final state at the LHC so far was made by the ATLAS Collaboration using the opening angle distributions between the decay products of the top quark and antiquark [11], giving $f = 1.12 \pm 0.11\,(\mathrm{stat}) \pm 0.22\,(\mathrm{syst})$ at $\sqrt{s} = 7\,\mathrm{TeV}$, using $4.6\,\mathrm{fb}^{-1}$ of integrated luminosity.

Here, a measurement of the top quark spin correlations in events characterised by the presence of a muon and jets (μ+jets) is described using a MEM at $\sqrt{s} = 8\,\mathrm{TeV}$ with $19.7\,\mathrm{fb}^{-1}$ of integrated luminosity. Events with a muon coming from a τ decay are not considered as part of the signal. In this analysis, the traditional discrete hypotheses are investigated: SM and uncorrelated $\mathrm{t\bar{t}}$ production and decay. In the MEM, the likelihood of an observed event to be produced by a given theoretical model is calculated. The likelihood ratio of the sample allows to distinguish between the two hypotheses. In addition, the distribution of event likelihood ratios is used in a template fit to extract the fraction f of events with the SM prediction of spin correlation.

The rest of this Letter is organised as follows. In Section 2, a description of the apparatus used in this measurement, the CMS detector, is given. Following, in Section 3, a description of the simulation samples used in this analysis is given. The event selection and reconstruction procedure of the physics objects in an event are given in Section 4. In Section 5, the MEM is briefly explained. Section 6 describes the first part of this analysis, the hypothesis-testing procedure, followed by the extraction of the variable f with a template fit in Section 7. The sources of systematic uncertainties are discussed in Section 8. A description on the treatment of these uncertainties in both parts of the analysis and the results are given in Section 9. Finally, a summary of the analysis is presented in Section 10.

2. The CMS detector

The central feature of the CMS apparatus [12] is a 3.8 T superconducting solenoid of 6 m internal diameter. The silicon pixel and strip tracker used for measuring charged-particle trajectories, a lead tungstate crystal electromagnetic calorimeter (ECAL), and the brass and scintillator hadron calorimeter (HCAL) are located within the superconducting solenoid volume. The calorimeters, ECAL and HCAL, both of which consist of a barrel and two endcap sections, surround the silicon tracking volume. Forward calorimetry extends the coverage provided by the barrel and endcap detectors to a pseudorapidity of $|\eta| = 5$.

Muons are measured using the tracker and the muon system that consists of gas-ionization detectors embedded in the steel flux-return yoke outside the solenoid. Muons are measured in the range $|\eta| < 2.4$, using three detector technologies: drift tubes, cathode strip chambers, and resistive-plate chambers. Matching muons to tracks measured in the silicon tracker results in a relative transverse momentum (p_{T}) resolution of 1.3–2.0% in the barrel and better than 6% in the endcaps for muons with $20 < p_{\mathrm{T}} < 100\,\mathrm{GeV}$. The p_{T} resolution in the barrel is better than 10% for muons with p_{T} up to 1 TeV [13].

The first level of the CMS trigger system, composed of custom hardware processors, uses information from the calorimeters and muon detectors to select the most interesting events. The high-level trigger processor farm further decreases the event rate from around 100 kHz to around 400 Hz, before data storage.

A more detailed description of the CMS detector, together with a definition of the coordinate system used, can be found in Ref. [12].

3. Signal and background modeling

The signal processes ($\mathrm{t\bar{t}}$ events in the μ+jets final state, SM and uncorrelated) as well as other $\mathrm{t\bar{t}}$ decay channels (SM and uncorrelated) are simulated on the basis of a next-to-leading-order (NLO) calculation using the generator MC@NLO v3.41 [14] with a top quark mass of 172.5 GeV. Parton showering is simulated using HERWIG 6.520 [15] and the default HERWIG6 underlying event tune was used. The NLO parton distribution function (PDF) set used is CTEQ6M [16]. The background samples of W+jets and Z/γ^{*}+jets processes are generated using MADGRAPH 5.1.3.30 [17], PYTHIA 6.426, and TAUOLA v27.121.5 [18]. The backgrounds from single top quark processes are generated using POWHEG v1 [19–21] and TAUOLA [22]. The Z2* underlying event tune is used. The most recent PYTHIA Z2* tune is derived from the Z1 tune [23], which uses the CTEQ5L parton distributions set, whereas Z2* adopts CTEQ6L [24]. The generated events are processed through the CMS detector simulation based on GEANT4 [25] and event reconstruction. To estimate the size of the effect of the top quark mass and factorisation and renormalisation scale uncertainties, MC@NLO samples with varied top quark mass and scales are used. The signal event yields are scaled to match the predicted top quark pair production cross section in proton–proton collisions at $\sqrt{s} = 8\,\mathrm{TeV}$, which is $\sigma_{\mathrm{t\bar{t}}}^{\mathrm{NNLO+NNLL}} = 245.8^{+6.2}_{-8.4}\,(\mathrm{scales})^{+6.2}_{-6.4}\,(\mathrm{PDF})\,\mathrm{pb}$ for a top quark mass equal to the world average of 173.3 GeV [26], computed with next-to-next-to-leading-order (NNLO) QCD corrections and next-to-next-to-leading-logarithmic (NNLL) resummation accuracy [27]. The simulated samples for the background processes are normalised using cross section calculations, generally at NLO accuracy [27]. Where necessary, systematically varied cross sections have been used for the normalisation. The simulation is corrected to the pileup conditions seen in the data. Pileup refers to the additional proton–proton interactions recorded simultaneously from the same bunch crossing. During 2012 data taking, there were on average 20 interactions per bunch crossing.

4. Event reconstruction and selection

The event selection has been optimised to identify $\mathrm{t\bar{t}}$ events in the μ+jets final state. A single-muon trigger with a muon p_{T} threshold of 24 GeV and a restriction on the pseudorapidity $|\eta| < 2.1$ is used to collect the data samples. Isolation and identification criteria are applied at the trigger level to achieve manageable rates with minimal loss of efficiency.

The physics objects used in this analysis are reconstructed with the CMS particle-flow (PF) algorithm [28,29]. The PF algorithm reconstructs and identifies each individual particle in an event using combined information from all CMS subdetectors. The energy of photons is directly obtained from the ECAL measurement. The energy of electrons is determined from a combination of the electron momentum measured at the primary interaction vertex by the tracker, the energy of the matched ECAL cluster, and the total energy of the associated bremsstrahlung photons. The momentum of muons is obtained from the curvature of the track associated to the muon. The energy of charged hadrons is determined from a combination of their momenta measured in the tracker and the matching energy deposits in the ECAL and HCAL, corrected for the calorimeter response to hadronic showers. Finally, the energy of neutral hadrons is obtained from the corresponding corrected ECAL and HCAL energy.

The reconstructed muon candidates are required to have $p_{\mathrm{T}} > 26\,\mathrm{GeV}$ and $|\eta| < 2.1$, as to be in a region where the trigger is fully efficient. The track associated to the muon candidate is required to have a minimum number of hits in the silicon tracker, to be consistent with the primary vertex, and to have a high-quality fit which combines a track in the tracker and a minimum number of hits in the muon detectors into one track. For each muon candidate, a PF-based relative isolation is calculated, corrected for pileup effects on an event-by-event basis. The transverse momenta of all reconstructed particle candidates (excluding the muon itself) are summed in a cone of size $\Delta R < 0.4$ around the muon direction, with $\Delta R = \sqrt{(\Delta\eta)^2 + (\Delta\phi)^2}$ where ϕ is the azimuthal angle expressed in radians. The pileup contribution in this scalar sum is corrected for by summing only over the charged particles associated to the event vertex in the charged particle contribution, and subtracting the average energy due to pileup in the neutral particle contribution. After subtraction of the pileup contribution, the scalar sum is required to be smaller than 12% of the muon p_{T}. It is required that exactly one of these well-identified muon candidates is present in the event. In addition, a looser selection on muons is applied which requires a relative isolation of less than 20% of the muon p_{T}, a selection of $p_{\mathrm{T}} > 10\,\mathrm{GeV}$ and $|\eta| < 2.5$. Events with additional muons passing looser identification criteria, as well as events with an electron are discarded. Events selected from other $\mathrm{t\bar{t}}$ final states are denoted as "$\mathrm{t\bar{t}}$ other" and consist of roughly 70% $\mathrm{t\bar{t}}$ events in the dilepton final state and 30% events in the τ+jets final state.

For each event, hadronic jets are clustered from the reconstructed particle-flow particles with the anti-k_{T} algorithm [30,31], with a distance parameter of 0.5. The jet momentum is determined as the vector sum of all particle momenta in the jet, which has been determined from simulation to be within 5% to 10% of the true momentum over the whole p_{T} spectrum and detector acceptance. Contributions from pileup are taken into account by an offset correction to the jet energies. Jet energy scale corrections (JES) up to particle-level are derived from simulation, and are confirmed with in-situ measurements of the energy balance in dijet and photon+jet events. The jet energy resolution (JER) in simulation is corrected to match the resolution observed in data. Additional selection criteria are applied to each event to remove spurious jet-like features originating from isolated uncharacteristic noise patterns in certain HCAL regions [32] and in the silicon avalanche photodiodes used in the ECAL barrel detector. The first three jets leading in p_{T} are required to have a p_{T} of at least 30 GeV, the fourth leading jet of at least 25 GeV and the remaining jets at least 20 GeV. At least two selected jets should be identified as coming from the decay of B-hadrons, based on the combined secondary vertex (CSV) algorithm with medium working point (CSVM) [33]. The CSV algorithm makes use of secondary vertices, when available, combined with track-based b-lifetime information. As the tracker coverage is limited to $|\eta| < 2.4$, all selected jets (both tagged and untagged) are restricted to this pseudorapidity range. The missing transverse momentum vector $\vec{p}_{\mathrm{T}}^{\,\mathrm{miss}}$ is defined as the projection on the plane perpendicular to the beams of the negative vector sum of the momenta of all reconstructed particles in an event. Its magnitude is referred to as $E_{\mathrm{T}}^{\mathrm{miss}}$. To reduce the effect of Final State Radiation (FSR), while not statistically limiting the analysis, we restrict the data set to events with four or five selected jets. To ensure that the selected jets in the event describe the $\mathrm{t\bar{t}}$ kinematic quantities, we reject events if they have additional forward jets in the region of $2.4 < |\eta| < 4.7$ and these have $p_{\mathrm{T}} > 50\,\mathrm{GeV}$.

Table 1
Event yield after event selection, with the statistical uncertainties. The contributions from various physics processes are given, with a comparison between the data and the total simulation at the bottom.

Process	Yield
W+jets	722 ± 20
Z/γ^*+jets	139 ± 18
$\mathrm{t}, \bar{\mathrm{t}}$ (s channel)	41 ± 3
$\mathrm{t}, \bar{\mathrm{t}}$ (t channel)	314 ± 10
$\mathrm{t}, \bar{\mathrm{t}}$ (tW)	935 ± 20
$\mathrm{t\bar{t}}$ other	3896 ± 24
$\mathrm{t\bar{t}}$ μ+jets	$31\,992 \pm 69$
Total simulation	$38\,039 \pm 81$
Data	37 775

To further increase the quality of the event selection and reduce the background contribution, we use a kinematic fitter, HitFit [34], designed to reconstruct the kinematic quantities of the $\mathrm{t\bar{t}}$ system in the lepton+jets final state. The kinematic quantities observed in the event are varied within the detector resolution to satisfy some predefined constraints, i.e. the reconstructed hadronically decaying W boson mass is required to be consistent with 80.4 GeV and the reconstructed top quark and antiquark masses are required to be equal. The HitFit algorithm tries every jet-quark permutation and the solution with the highest goodness-of-fit (or equivalently, lowest χ^2/ndof with ndof being the number of degrees of freedom) is chosen as the best estimate of the correct jet-quark permutation. We do not rely on HitFit to estimate the jet-quark permutation correctly, however, HitFit is used to decide which four jets in the event to use in the reconstruction of the $\mathrm{t\bar{t}}$ final state in five-jet events. It is required that two of the jets selected by HitFit are identified as originating from B-hadrons. The selection of the jets in the event could be done with simpler methods, e.g. selecting the highest-p_{T} jets, but HitFit offers the possibility to apply additional quality criteria. In order to reduce the background fraction and the fraction of mismodeled events, we only select events with a HitFit χ^2/ndof < 5 or, equivalently, with the fit probability larger than 0.08. The value of the χ^2/ndof-selection is chosen to maximise the separation power defined by Eq. (7) in Section 6. Mismodeled events can be due to the inclusion of radiated jets in the $\mathrm{t\bar{t}}$ reconstruction or events with poorly reconstructed jet quantities. The χ^2 probability distribution is shown for data and simulation in Fig. 1, where the relative contributions of the simulation are determined from the theoretical cross sections.

The event yield after the full event selection is displayed in Table 1. The contributions are estimated from simulation and normalised to the observed luminosity using theoretical cross sections. The selection efficiency for the SM and uncorrelated signal samples are very similar so that the event selection does not bias the data towards one hypothesis. The background contribution due to multijet processes has been estimated from simulation and is found to be negligible.

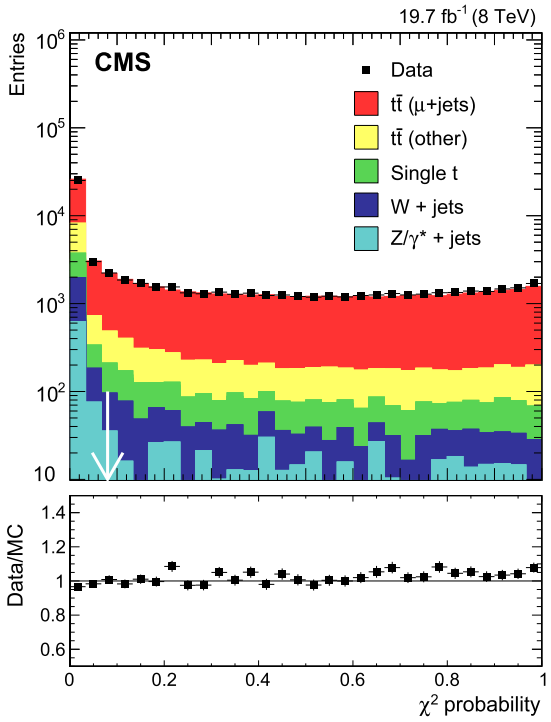

Fig. 1. The χ^2 probability distribution of the selected solutions of the kinematic fit in the μ+jets channel, showing a shape comparison between data and simulation including the statistical uncertainties. The relative contributions in simulation are calculated using the theoretical cross sections with the total yield normalised to data. For the analysis, we only consider events with a probability larger than 0.08, as indicated by the arrow.

5. Matrix element method

The matrix element method [35–38] is a technique that directly relates theory with experimental events. The compatibility of the data recorded with the leading-order (LO) matrix element (ME) of a certain process is evaluated. The probability that an event is produced by this process is calculated using the full kinematic information in the event.

The probability $P(x_i|H)$ to observe an event i with kinematic properties x for a certain hypothesis H is given by:

$$P(x_i|H) = \frac{1}{\sigma_{\text{obs}}(H)} \int f_{\text{PDF}}(q_1) f_{\text{PDF}}(q_2) \mathrm{d}q_1 \mathrm{d}q_2 \frac{(2\pi)^4 |M(y,H)|^2}{q_1 q_2 s} W(x_i, y) \mathrm{d}\Phi_6. \quad (3)$$

The given probability is equivalent to an event likelihood. In this equation, q_1 and q_2 represent the parton energy fractions in the collision, $f_{\text{PDF}}(q_1)$ and $f_{\text{PDF}}(q_2)$ are the PDFs, s is the centre-of-mass energy squared of the colliding protons, and $\mathrm{d}\Phi_6$ represents the phase space volume element. The transfer function, $W(x, y)$, relates observed kinematic quantities x with parton-level quantities y. For every y, the transfer function is normalised to unity by integrating over all possible values of x. The LO ME is represented by $M(y, H)$, where H denotes the hypothesis used. The $\mathrm{t\bar{t}}$ spin correlation strength is not a parameter of the SM Lagrangian, therefore H is not a continuous parameter. The MEs $M(y, H_{\text{cor}})$ and $M(y, H_{\text{uncor}})$ both describe $\mathrm{t\bar{t}}$ production and subsequent decay in the μ+jets channel valid for both on- and off-shell top quarks. In this analysis, the hypotheses are either the SM (H_{cor}), giving rise to a finite value of the spin correlation strength A (as discussed in Section 1) or the spin-uncorrelated hypothesis with $A = 0$ (H_{uncor}). Finally, $\sigma_{\text{obs}}(H)$ represents the observed $\mathrm{t\bar{t}}$ cross section of the hypothesis, which ensures that the probability is normalised. The quantity $\sigma_{\text{obs}}(H)$ consists of the product of the production cross section σ, which is identical for our considered hypotheses, and the overall selection efficiency $\epsilon(H)$. The selection efficiency for events from both hypotheses are very similar, with an efficiency of $\epsilon(SM) = 0.0448 \pm 0.0001\,(\text{stat})$ for the SM $t\bar{t}$ signal hypothesis, and $\epsilon(uncor) = 0.0458 \pm 0.0001\,(\text{stat})$ for the uncorrelated signal hypothesis, which causes acceptance effects to nearly cancel in the likelihood ratio. The likelihood calculation is performed using MadWeight [39], in the MadGraph5 framework [17]. Since, in our convention, the likelihood for a single event is represented by $P(x_i|H)$, the likelihood of a sample with n events is then

$$L(x_1, \ldots, x_n|H) = \Pi_{i=1}^{n} P(x_i|H). \quad (4)$$

The transfer function of a given interacting particle depends on the specifics of the detector. In this analysis, the transfer function is used to correct the jet kinematic quantities. The reconstructed jet energy information, corrected for JES and JER, is mapped onto parton-level quantities by integrating over the parton energy within the transfer function resolution during the likelihood calculation. All other kinematic quantities (such as angular information or lepton quantities) are unmodified by the transfer function as these are measured with sufficient accuracy with the CMS detector to describe a final state that does not include a dilepton resonance. The description of these variables with a Dirac delta function speeds up the integration. The $E_{\text{T}}^{\text{miss}}$ is also described with a Dirac delta function and is only used to correct the kinematic quantities of the event for the transverse Lorentz boost. The event transfer function is the product of the object transfer functions, assuming no correlation between the reconstructed objects. The jet energy transfer function is determined from $\mathrm{t\bar{t}}$ simulation to which the JES and JER corrections have been applied. For each jet in the simulation, unambiguously matched to a parton with $\Delta R(\text{jet}, \text{parton}) < 0.3$, the E_{jet} and E_{parton} are compared (separately for jets matched to b and light-flavour partons). The E_{jet} distribution is fitted with a Gaussian function, where the Gaussian mean and width depend on E_{parton} and are given by $\mu(E_{\text{jet}}) = m_0(\eta_{\text{parton}}) + m_1(\eta_{\text{parton}}) E_{\text{parton}}$ and $\sigma(E_{\text{jet}}) = \sigma_0(\eta_{\text{parton}}) + \sigma_1(\eta_{\text{parton}}) E_{\text{parton}} + \sigma_2(\eta_{\text{parton}}) \sqrt{E_{\text{parton}}}$ respectively. The fit of the E_{jet} distribution is converted to a single Gaussian transfer function, which is a function of the variable $\Delta E = E_{\text{parton}} - E_{\text{jet}}$ and the parameters are a function of E_{parton}. The transfer function, which is determined in the full kinematic phase space, is given by

$$W(E_{\text{parton}}, E_{\text{jet}}) = \frac{1}{\sqrt{2\pi}\left(\sigma_0 + \sigma_1 E_{\text{parton}} + \sigma_2 \sqrt{E_{\text{parton}}}\right)} \times \exp\left[-\frac{1}{2}\left(\frac{\Delta E + m_0 + m_1 E_{\text{parton}}}{\sigma_0 + \sigma_1 E_{\text{parton}} + \sigma_2 \sqrt{E_{\text{parton}}}}\right)^2\right], \quad (5)$$

where the parameters are determined independently for b jets and light-flavour jets, in three slices of $|\eta_{\text{parton}}|$ given by $0 < |\eta_{\text{parton}}| < 0.87$, $0.87 < |\eta_{\text{parton}}| < 1.48$ and $1.48 < |\eta_{\text{parton}}| < 2.5$. In Fig. 2, the ΔE distribution is shown for the $\Delta E = E_{\text{parton}} - E_{\text{jet}}$ from simulation for all values of E_{parton} and $|\eta_{\text{parton}}|$. This is compared to the ΔE distribution obtained by folding the E_{parton} spectrum of matched partons with the transfer function. The reasonably good agreement of the resolution and the tails of the two distributions shows that the determined transfer functions are adequate.

The disadvantage of using a LO ME is that there is no explicit treatment for final state radiation in the MEs. As a result, the ME does not always cover the full event information leading

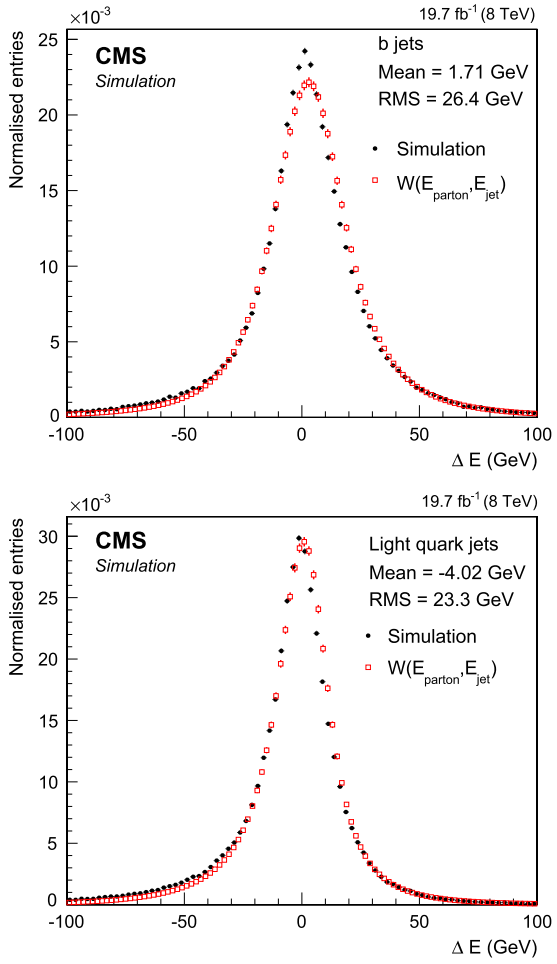

Fig. 2. ΔE distributions based on the values obtained from simulation (circles) compared to the ΔE distribution obtained by folding the E_{parton} spectrum of matched partons with the transfer function (squares) summed over all values of E_{parton} and $|\eta_{\text{parton}}|$. The mean and RMS shown on the plots are obtained from simulation. The figure is shown for b quark jets (top) and for light quark jets (bottom).

to a slightly reduced discrimination between both hypotheses. In addition, background events evaluated under a $\mathrm{t\bar{t}}$ hypothesis will more closely resemble the uncorrelated hypothesis as there is no correlation between the decay products. In the template fit part of this analysis, the small bias due to this effect is corrected for with a calibration curve (described in Section 7), whereas in the hypothesis testing the background contribution is fixed to the predictions from simulation, so no bias is present. MadWeight [39], the tool used to perform the MEM likelihood calculations, can partially correct for the initial state radiation (ISR) effect by evaluating the LO ME at an overall partonic p_{T} of the $\mathrm{t\bar{t}}$ system equal to the reconstructed p_{T} of the system, thus properly treating five-jet events where one jet is due to ISR. Due to final state radiation (FSR), the matching with the LO ME, which requires four jets as input, becomes more difficult and more sensitive to systematic uncertainties related to variations on the jet energy scale or on the renormalisation/factorisation scales. The $\mathrm{t\bar{t}}$ system is reconstructed using the four selected jets based on HitFit in the event, the lepton and the $\vec{p}_{\mathrm{T}}^{\,\mathrm{miss}}$. The $\vec{p}_{\mathrm{T}}^{\,\mathrm{miss}}$ quantity is assigned to the undetected neutrino from the $\mathrm{t\bar{t}}$ muon+jets final state. In the MadWeight likelihood calculations, every jet-quark permutation compatible with b tagging information is taken into account.

6. Hypothesis testing

The compatibility of the data with the SM hypothesis and the fully uncorrelated hypothesis is tested. The likelihood for each event is calculated under these two hypotheses, as described in Section 5. According to the Neyman–Pearson lemma, the test statistic with maximum separation power for a sample coming from either of two simple hypotheses is the likelihood ratio. This analysis uses λ_{event} as the discriminating variable, defined as

$$\lambda_{\text{event}} = \frac{P(H_{\text{uncor}})}{P(H_{\text{cor}})}, \tag{6}$$

where $P(H_{\text{cor}})$ is the likelihood for the event under the SM hypothesis and similarly $P(H_{\text{uncor}})$ for the uncorrelated hypothesis.

Following the prescription proposed by Cousins et al. [40], we use $-2\ln\lambda_{\text{event}}$ as test statistic, a quantity hereafter referred to as the event likelihood ratio. The distributions of $-2\ln\lambda_{\text{event}}$ are shown in Fig. 3 for the SM $\mathrm{t\bar{t}}$ sample (Fig. 3-top) and the uncorrelated $\mathrm{t\bar{t}}$ sample (Fig. 3-bottom). The plots show a shape comparison between data and simulation. The differences between the SM and uncorrelated distribution are statistically significant. The expected distribution of the sample likelihood ratio, defined as $-2\ln\lambda_{\text{sample}} = -\Sigma 2\ln\lambda_{\text{event}}$, is calculated by drawing pseudo-experiments with the data sample size. In the pseudo-experiments, the relative signal and background ratios are kept fixed based on the theoretical cross sections. These pseudo-experiments are performed with the SM and uncorrelated event likelihood ratio distributions, respectively. The bin width of the event likelihood ratio distribution is chosen as 0.14 and the range of the distribution used is $[-0.70, 1.26]$. Events outside this $-2\ln\lambda_{\text{event}}$ range of $[-0.70, 1.26]$ are discarded. The shape differences of the $-2\ln\lambda_{\text{event}}$ distribution between the SM and uncorrelated signal hypothesis outside of this range are not statistically significant. The distribution of the sample likelihood ratios, using pseudo-experiments drawn at the data set size of 36 800 events within the range $-2\ln\lambda_{\text{event}} = [-0.70, 1.26]$, is shown in Fig. 4. The solid line shows the expected Gaussian distribution of the sample likelihood ratios for this size using the SM $\mathrm{t\bar{t}}$ simulation as signal and the dashed line shows the Gaussian distribution using the uncorrelated $\mathrm{t\bar{t}}$ simulation as signal. A way of quantifying the overlap between the sample likelihood ratio distributions of the two hypotheses is given by the separation power

$$S = \frac{\mu_1 - \mu_2}{\sqrt{\alpha_1^2 + \alpha_2^2}}, \tag{7}$$

with $\mu_{1,2}$ being the means of the distributions and $\alpha_{1,2}$ their width [40]. The separation power is a measure for the discrimination obtainable, for the size of the data set, between the two hypotheses expressed in standard deviations (σ). Fig. 4 shows that a separation power of 8.8 σ can be obtained with the MEM when only statistical effects are taken into account. The distributions will be modified by the inclusion of the systematic uncertainties described in Section 8. The range of the $-2\ln\lambda_{\text{event}}$ distribution is chosen to maximise the separation power, while the binning is chosen finely enough to preserve the available separation power. In addition, the event selection (in particular the selection on the HitFit χ^2/ndof) has been optimised to maximise the separation power.

7. Extraction of fraction of events with SM spin correlation

We extract the fraction f of $\mathrm{t\bar{t}}$ signal events with the SM spin correlation by performing a template fit to the $-2\ln\lambda_{\text{event}}$ distribution. The fit model $M(f_{\text{obs}}, \beta_{\text{obs}})$ is given by

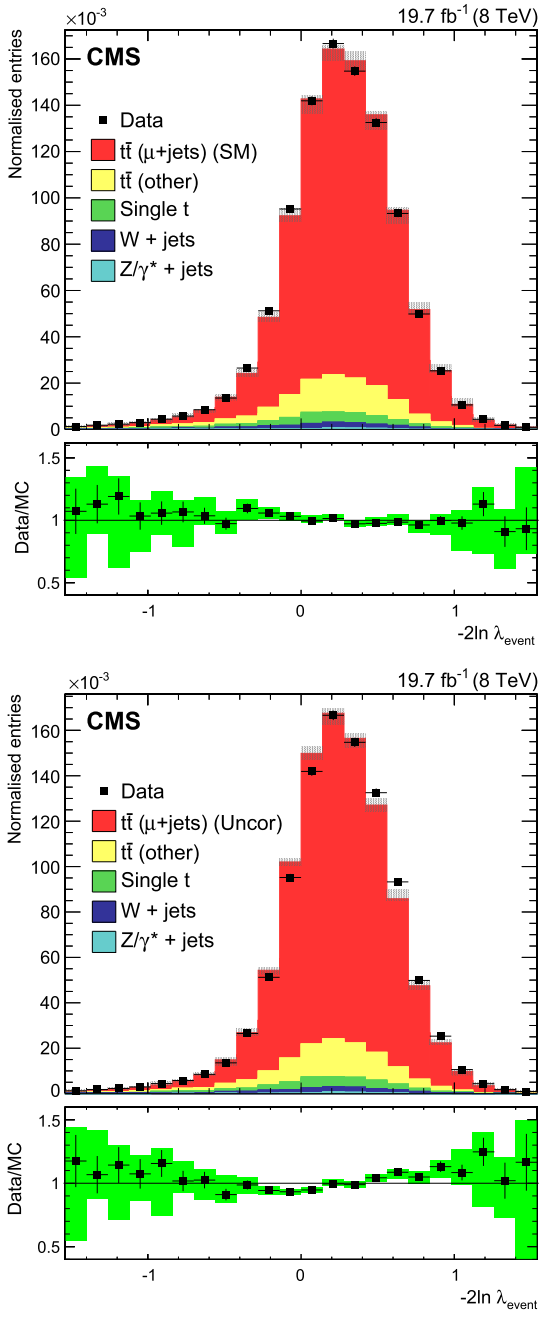

Fig. 3. Distribution of $-2\ln\lambda_{\text{event}}$. The SM $t\bar{t}$ simulation is used in the top plot and the uncorrelated $t\bar{t}$ simulation in the bottom plot. Both data and simulation are normalised to unity. The hatched uncertainty band includes statistical and systematic uncertainties. The error bars in the ratio plot at the bottom only consider statistical uncertainties (of both data and simulation), while the uncertainty band covers both statistical and systematic uncertainties. Systematic uncertainties are described in Section 8. The overlap of the green uncertainty band, which is constructed around the marker position, with the ratio value of 1 indicates agreement between the data and the simulation within the total uncertainty.

$$M(f_{\text{obs}},\beta_{\text{obs}}) = (1-\beta_{\text{obs}})\,[f_{\text{obs}}\,T_{\text{cor}} + (1-f_{\text{obs}})\,T_{\text{uncor}}] + \beta_{\text{obs}}\,T_{\text{bkg}}, \tag{8}$$

where f_{obs} is the fraction of events with the SM spin correlation, and β_{obs} is the fraction of background in the data. The $t\bar{t}$ signal SM template, the $t\bar{t}$ signal uncorrelated template, and the background template are denoted by T_{cor}, T_{uncor}, and T_{bkg}, respectively. The

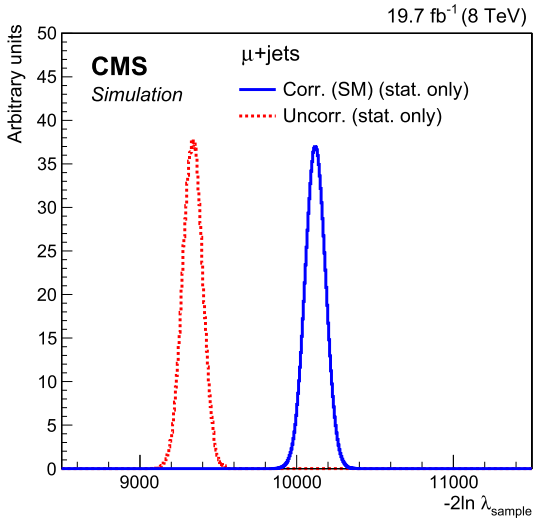

Fig. 4. The expected $-2\ln\lambda_{\text{sample}}$ distribution estimated using simulation, evaluated at the data sample size. The samples in simulation contain signal and background mixed according to the theoretical cross sections, with the solid Gaussian function using SM $t\bar{t}$ simulation and the dashed Gaussian function using uncorrelated $t\bar{t}$ simulation. From this figure, the separation power can be assessed in the case when systematic effects are not considered.

background template contains the averaged contribution of the $t\bar{t}$ other background with SM spin correlation and the $t\bar{t}$ other with no spin correlation as these contributions are the same within statistical uncertainties. Systematic uncertainties are not included in the fit model. The parameter estimation is done using a binned maximum likelihood fit in RooFit [41], using Minuit [42]. The total normalisation is fixed to the observed data yield, but the relative background contribution and the fraction f_{obs} are allowed to vary unconstrained in the fit. The binning and range of the template distributions are fixed to those used in the hypothesis testing, where they have been chosen to optimize the separation power between the two hypotheses.

There is a small bias in the extraction of f_{obs} in the template fit due to the presence of background in the sample. The background shape resembles more the behaviour of the uncorrelated template, and the size of the sample from which the background template is derived is small. The small bias is corrected for with a calibration function. The bias is estimated from the simulation via pseudo-experiments with the observed data set size for a range of working points (f_{input}, β_{input}). At each working point, the mean observed f_{obs} and β_{obs} are extracted to construct a 2D calibration function, used to derive $f_{\text{calibrated}}$ as a function of the observed f_{obs} and β_{obs}. The f_{obs}- and β_{obs}-variables have been shifted by the weighted average of the evaluated working points to decorrelate the fit parameters. The calibration function is given by

$$f = p_0 + p_1\,f'_{\text{obs}} + p_2\,f'_{\text{obs}}\,\beta'_{\text{obs}}, \tag{9}$$

with $f'_{\text{obs}} = f_{\text{obs}} - 0.502$ and $\beta'_{\text{obs}} = \beta_{\text{obs}} - 0.150$. The fit parameters of the calibration function are listed in Table 2.

Table 2
Fit parameters of the 2D calibration function. The residual correlation between the fit parameters is below 10% and is ignored.

Parameter	Value
p_0	0.5004 ± 0.0003
p_1	0.9207 ± 0.0008
p_2	-0.56 ± 0.01
χ^2/ndof	80/95

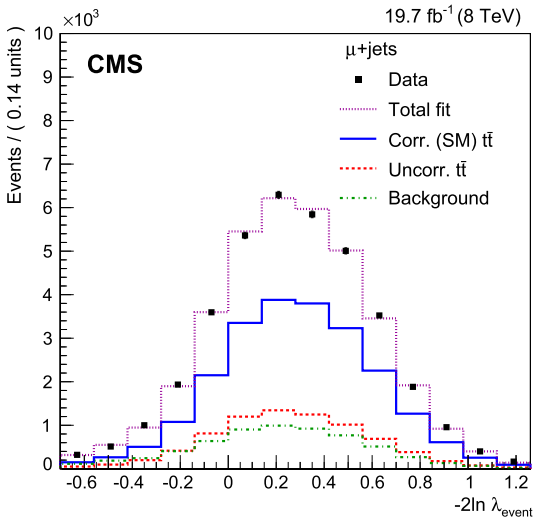

Fig. 5. Result of the template fit to data. The squares represent the data with the statistical uncertainty smaller than the marker size, the dotted curve is the overall result of the fit, the solid curve is the contribution of the SM signal template to the fit, the dashed curve is the contribution of the uncorrelated signal, and the dash–dot curve is the background contribution.

It has been checked that the initial values of the parameters in the fit model have no influence on the template fit result. The result of the template fit on the data is shown in Fig. 5 with $f_{\text{obs,data}} = 0.747 \pm 0.092$, $\beta_{\text{obs,data}} = 0.168 \pm 0.024$, and a $\chi^2/\text{ndof} = 1.552$. From simulation, a background fraction β of 15.5% is expected in the fit range. After calibration of both the nominal result and the statistical uncertainty, the result is:

$$f = 0.724 \pm 0.084\,(\text{stat}). \tag{10}$$

In the fit to the $-2\ln\lambda_{\text{event}}$ distribution in the range $[-0.7, 1.26]$, the correlation between $f_{\text{obs,data}}$ and $\beta_{\text{obs,data}}$ is around 54%.

8. Sources of systematic uncertainty

Systematic uncertainties affecting this analysis come from various sources, such as detector effects, theoretical uncertainties, and mismodeling in the simulation. The simulation is corrected where necessary by the use of event weights to account for efficiency differences in the data and simulation, e.g. muon identification, isolation efficiency, trigger efficiencies, b tagging and mistagging rates and pileup modeling. The systematic uncertainties are determined, independently of each other, by varying the efficiency correction, resolution, or scale correction factors within their uncertainties. For some uncertainties, this is equivalent to varying the event weights, for others, this requires recalculating the event likelihoods. In both cases, the $-2\ln\lambda_{\text{event}}$ distributions from which pseudo-experiments are drawn to calculate the sample likelihood ratios in simulation or that are used as templates for the fit, are modified. The sources of systematic uncertainties common to the hypothesis testing and template fit are listed and explained below. The order of the list of contributions gives an indication of the relative importance of the contribution in both the template fit and the hypothesis testing. The explicit treatment of the systematic uncertainties is explained in more detail in Section 9.1 for the hypothesis testing and in Section 9.2 for the template fit.

Limited statistical precision of simulation: The $-2\ln\lambda_{\text{event}}$ distributions are obtained from simulation with finite statistical precision. To estimate the effect of the statistical precision in this distribution on the observed significance or on the template fit, each bin of the $-2\ln\lambda_{\text{event}}$ distribution is varied randomly using a Poisson distribution within the statistical uncertainties. This is done independently for each simulation sample that contributes to the $-2\ln\lambda_{\text{event}}$ distribution.

Scale uncertainty: SM and uncorrelated $t\bar{t}$ samples with varied renormalisation and factorisation scales are used to estimate the uncertainty caused by the scale uncertainty. The renormalisation and factorisation scales are simultaneously doubled or halved with respect to their nominal values set to the sum of the transverse masses squared of the final-state particles (in the case of $t\bar{t}$ events this is the top quark pair and any additional parton) divided by two. The effect of the scale variation on the event selection is included.

JES and JER effects: The four-momenta of all jets reconstructed in simulated events are varied simultaneously within the uncertainties of the p_{T}- and η-dependent JES [43,44] prior to the event selection. The additional resolution correction applied to the simulation to take into account the resolution difference between data and simulation is varied within the uncertainties in the simulation. The likelihood calculations are performed with the varied jet quantities, using the nominal transfer function. The JES uncertainty enters the measurement in two ways: (i) acceptance effects modify the relative contributions of the backgrounds and (ii) the event likelihood values vary due to the modified quantities. The latter effect is dominant.

Parton distribution functions: The PDF is varied within its uncertainty eigenvectors (CT10) in signal and background, and the effects are propagated through the event weights [45,46]. The procedure to propagate the effect to the $-2\ln\lambda_{\text{event}}$ distribution is described in [45].

Top quark mass uncertainty: SM and uncorrelated $t\bar{t}$ samples with varied top quark mass values have been produced, including the effect on the event selection. The nominal sample is simulated with a top quark mass of 172.5 GeV, whereas the systematically varied samples are simulated with $m_{\text{t}} = 169.5$ GeV and $m_{\text{t}} = 175.5$ GeV. The $-2\ln\lambda_{\text{event}}$ distribution is varied within 1/3 of the deviation obtained with $m_{\text{t}} = 175.5$ GeV and $m_{\text{t}} = 169.5$ GeV in order to mimic the $-2\ln\lambda_{\text{event}}$ variation caused by a 1 GeV uncertainty in the top quark mass world average value [26].

The top quark p_{T}^{t} modeling: The model of $t\bar{t}$ production in MadGraph as well as in mc@nlo predicts a harder transverse momentum spectrum for the top quark p_{T}^{t} than observed in the data [47,48]. The top quark pairs might be reweighted based on the p_{T} spectrum of generator-level top quarks to obtain better agreement to the measured differential cross section. This reweighting is not applied in this analysis, but we do assign an uncertainty to the $t\bar{t}$ modeling by changing the event weight and propagating the effect to the $-2\ln\lambda_{\text{event}}$ shape.

Background modeling and theoretical cross sections: We determine the relative contribution of the backgrounds using the theoretical cross sections for the background processes. The cross sections are varied within the theoretical uncertainties [27] and the effects are propagated to the analysis. The total background shape will change due to the change in relative contributions and, in the hypothesis testing, the total background fraction is fixed to the systematically varied value, whereas in the template fit, this fraction can vary freely in the fit. For the W+jets contribution, we vary the background yield by 50% and propagate the effects to the analysis, which is ample to cover the uncertainties on the theoretical cross sections. The shape of the W+jets background template is also varied by evaluating the $-2\ln\lambda_{\text{event}}$ distribution without the W+jets shape included, but keeping the total background fraction fixed to the nominal value.

Pileup: A 5% uncertainty on the inelastic pp cross section is taken into account and propagated to the event weights [49].

The b tagging efficiency and mistag rates: The p_T- and η-dependent tagging and mistagging efficiencies for light- and heavy-flavour jets are varied within their uncertainties and are propagated to the event weights in the simulation [50].

Lepton trigger, identification, and isolation efficiencies: p_T- and η-dependent scale factors are applied to the simulation to correct for efficiency differences in the data and simulation for the single lepton trigger, lepton identification and isolation. These scale factors are varied independently within their uncertainties and the effects are propagated to the event weights.

The contribution of the individual systematic uncertainty sources is evaluated in the template fitting procedure described in Section 9.2 and reported in Table 3. The relative size of each systematic uncertainty contribution is consistent in the hypothesis testing procedure and the template fitting.

9. Results

9.1. Hypothesis testing

To evaluate the compatibility of the data with either of the hypotheses, the systematic variations of the $-2\ln\lambda_{\text{event}}$ distribution need to be propagated to the $-2\ln\lambda_{\text{sample}}$ distribution. We assess the effect of this event likelihood ratio fluctuation by a Gaussian template morphing technique in which all systematic uncertainties are evaluated simultaneously. In each pseudo-experiment, we draw a sample from the morphed template with a size equal to that of the data set, and evaluate the sample likelihood ratio.

The $-2\ln\lambda_{\text{event}}$ distribution is morphed in the following way. We draw a vector $\vec{x}$ of random numbers from a Gaussian distribution with mean 0 and width 1. Per systematic uncertainty source k, we have an independent entry x_k in the vector. In each bin of the morphed template, the bin content N_i is calculated as shown in the following equation with $H(x_k)$ a Heaviside step function and N_i^{nom} the original bin content:

$$N_i = N_i^{\text{nom}} + \Sigma_k |x_k| \left(H(x_k) \left[N_i^{k,\text{up}} - N_i^{\text{nom}} \right] + H(-x_k) \left[N_i^{k,\text{down}} - N_i^{\text{nom}} \right] \right). \tag{11}$$

Here, $N^{k,\text{up}}$ and $N^{k,\text{down}}$ are the bin contents of the systematically varied $-2\ln\lambda_{\text{event}}$ distribution for the upward and downward variation respectively. The summation runs over all systematic uncertainty sources. The systematic upward fluctuation is chosen for a systematic source when x_k is positive and the downward fluctuation is chosen when x_k is negative. This equation shows that all systematic uncertainty sources are varied simultaneously while the bin-to-bin correlations of the systematic effect is preserved. If the systematic up- and down-effects are asymmetric in size, this asymmetry is preserved. If the systematic up- and down-effects give a change in the same direction, the largest of the two contributions is chosen as a one-sided uncertainty while zero is used for the opposite side. Per template morphing iteration, we draw one $\vec{x}$ which gives us a varied $-2\ln\lambda_{\text{event}}$ distribution. From this distribution with this particular $\vec{x}$, we draw one pseudo-experiment with a size equal to that of the data set. This is done independently for the SM and uncorrelated $-2\ln\lambda_{\text{event}}$ distribution.

We perform repeated pseudo-experiments with the template morphing technique to obtain the systematically varied sample likelihood ratio distribution shown in Fig. 6. The comparison of Figs. 4 and 6 shows the degradation of the separation power between the SM distribution and the uncorrelated distribution due to the systematic uncertainties. In addition, the result of the asymmetric behaviour of some systematic uncertainty sources is clearly visible. Performing 10^7 pseudo-experiments is enough to populate the Gaussian tails in the template morphing phase space, ensuring a smooth $-2\ln\lambda_{\text{sample}}$ distribution with low statistical uncertainty even in the tails.

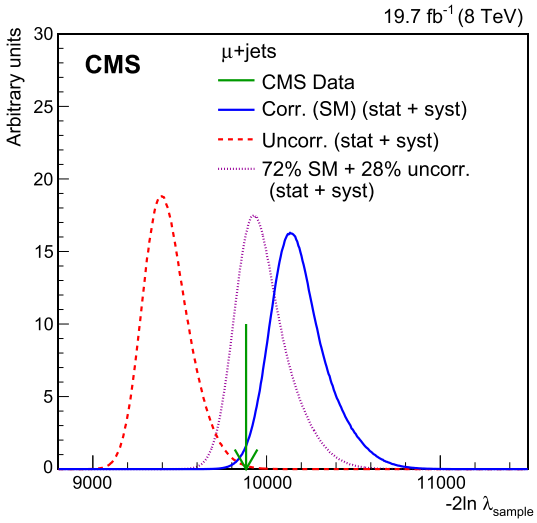

Fig. 6. The $-2\ln\lambda_{\text{sample}}$ distribution in simulation, evaluated for the data set size. The samples in simulation contain signal and background mixed according to the theoretical cross sections, with the solid distribution obtained using SM $t\bar{t}$ simulation and the dashed distribution obtained using uncorrelated $t\bar{t}$ simulation, including systematic uncertainties. The arrow indicates the $-2\ln\lambda_{\text{sample}}$ observed in data. The dotted curve shows a mixture of 72% SM $t\bar{t}$ events and 28% uncorrelated $t\bar{t}$ events.

From the value of the data sample likelihood ratio, we find that 98.7% of the SM simulated area is above the data value, leading to an observed agreement with the SM hypothesis of 2.2 standard deviations. We find that 0.2% of the uncorrelated simulated area is above the data value, leading to an observed agreement of the uncorrelated hypothesis of 2.9 standard deviations. From this we can conclude that the data is more compatible with the SM hypothesis than with the uncorrelated hypothesis. The dominant uncertainty sources are the JES, scale variation, and the top quark mass uncertainties. The JES uncertainty is responsible for the asymmetric tails in the distribution.

As a test of the compatibility of the result in the hypothesis testing and the extraction of f, the hypothesis testing has been performed with a $t\bar{t}$ sample constructed such that 72% of the events contained SM correlations while the remainder 28% had no correlation. As a result we find a sample likelihood ratio distribution, shown in Fig. 6, in between the SM and uncorrelated scenario, with a data compatibility of 0.6 standard deviations. The value measured in data, which is slightly below the mean of the distribution, is within the expectation of statistical and systematic effects. We would have achieved even better agreement had we used in simulation a value of the top quark mass equal to the world average measurement of 173.3 GeV [26].

9.2. Extraction of fraction of events with SM spin correlation

In the extraction of f using a template fit to the variable $-2\ln\lambda_{\text{event}}$, we have the same list of systematic uncertainty sources as described earlier, but in addition a systematic uncertainty due to the calibration of the method is taken into account. The calibration uncertainty is obtained by propagating the uncertainties in the calibration fit parameters shown in Table 2 and propagating the fit uncertainty of the fit parameter $\beta_{\text{obs,data}}$.

The systematic uncertainties are determined by fitting the data with systematically varied templates and taking the difference from the nominal fit result. The systematic contributions, taking

Table 3
Sources of systematic uncertainty in the fraction f of events with the SM spin correlation. There is no downward variation for the p_T^t modeling.

Source of syst. uncer.	Up variation	Down variation
Simulation stat.	0.042	−0.042
Scale	−0.068	0.124
JES	0.051	−0.090
JER	−0.023	−0.004
PDF	0.018	0.045
m_t	0.001	−0.034
top quark p_T^t modeling	0.023	–
Background modeling	0.017	−0.016
Pileup	0.012	−0.015
b tagging efficiency	−0.001	0.001
Mistag rate	0.005	−0.006
Trigger	<0.001	<0.001
Lepton ID/Iso	<0.001	<0.001
Calibration	0.003	−0.003
Total syst. uncer.	$^{+0.15}_{-0.13}$	

into account the effect of the nominal calibration function, are shown in Table 3 where the fit uncertainty of the nominal result is also shown. The systematic uncertainty related to the finite size of the simulation samples is evaluated by fitting one pseudo-data set in the simulation by 1000 Poisson-fluctuated templates. The Gaussian width of the fit result f_{obs} is taken as the systematic uncertainty value. This is done for each simulation sample independently with the uncertainties added in quadrature. In the template fit method, all systematic uncertainties are treated as independent of each other.

The total systematic uncertainty is obtained by adding the positive and negative contributions in Table 3 in quadrature. When both up and down systematic variations give an uncertainty in the same direction, only the largest value is taken into account in the given direction, and no uncertainty is assigned in the opposite direction. This gives us a total systematic uncertainty of +0.15 and −0.13. The total result of the template fit is then:

$$f = 0.72 \pm 0.08\,(\text{stat})^{+0.15}_{-0.13}\,(\text{syst}). \tag{12}$$

In the assumption that there are only the SM $t\bar{t}$ pairs or uncorrelated $t\bar{t}$ pairs, this results in an indirect extraction of A_{hel}. By making use of the relation $A_{hel}^{measured} = f^{SM} A_{hel}^{SM,MC}$ where $A_{hel}^{SM,MC} = 0.324 \pm 0.003$ obtained in simulation, which is in good agreement with the theoretically predicted value of $A_{hel}^{SM} = 0.319$ [51,52] which includes NLO QCD and electroweak corrections, $A_{hel}^{measured} = 0.23 \pm 0.03\,(\text{stat})^{+0.05}_{-0.04}\,(\text{syst})$ is obtained. It is found that the systematic uncertainties due to JER, trigger, lepton identification and isolation efficiencies, and b tagging efficiency are not relevant compared to the statistical uncertainties associated to them. The dominant uncertainties are the JES and renormalisation/factorisation scale variation. The relative contributions of systematic uncertainty are very similar in the hypothesis testing and template fit results.

10. Summary

The hypothesis that $t\bar{t}$ events are produced with correlated spins as predicted by the SM is tested using a matrix element method in the μ+jets final state at $\sqrt{s} = 8$ TeV, using pp collisions corresponding to an integrated luminosity of 19.7 fb^{-1}. The data agree with the uncorrelated hypothesis within 2.9 standard deviations, whereas agreement with the SM is within 2.2 standard deviations. Our hypotheses are only considered up to NLO effects in the simulation, with LO matrix elements in the likelihood calculations.

Using a template fit method, the fraction of events which show SM spin correlations has been extracted. This fraction is measured to be $f = 0.72 \pm 0.08\,(\text{stat})^{+0.15}_{-0.13}\,(\text{syst})$, leading to a spin correlation strength of $A_{hel}^{measured} = 0.23 \pm 0.03\,(\text{stat})^{+0.05}_{-0.04}\,(\text{syst})$ using the value obtained in simulation which is compatible with the theoretical prediction for A_{hel}^{SM} from [51,52]. The result is the most precise determination of this quantity in the muon+jets final state to date and is competitive with the most accurate result in the dilepton final state [9].

Acknowledgements

We thank Werner Bernreuther for kindly providing the LO matrix elements describing $t\bar{t}$ production and subsequent decay in the μ+jets channel, valid for both on- and off-shell top quarks.

We congratulate our colleagues in the CERN accelerator departments for the excellent performance of the LHC and thank the technical and administrative staffs at CERN and at other CMS institutes for their contributions to the success of the CMS effort. In addition, we gratefully acknowledge the computing centres and personnel of the Worldwide LHC Computing Grid for delivering so effectively the computing infrastructure essential to our analyses. Finally, we acknowledge the enduring support for the construction and operation of the LHC and the CMS detector provided by the following funding agencies: BMWFW and FWF (Austria); FNRS and FWO (Belgium); CNPq, CAPES, FAPERJ, and FAPESP (Brazil); MES (Bulgaria); CERN; CAS, MoST, and NSFC (China); COLCIENCIAS (Colombia); MSES and CSF (Croatia); RPF (Cyprus); MoER, ERC IUT and ERDF (Estonia); Academy of Finland, MEC, and HIP (Finland); CEA and CNRS/IN2P3 (France); BMBF, DFG, and HGF (Germany); GSRT (Greece); OTKA and NIH (Hungary); DAE and DST (India); IPM (Iran); SFI (Ireland); INFN (Italy); MSIP and NRF (Republic of Korea); LAS (Lithuania); MOE and UM (Malaysia); CINVESTAV, CONACYT, SEP, and UASLP-FAI (Mexico); MBIE (New Zealand); PAEC (Pakistan); MSHE and NSC (Poland); FCT (Portugal); JINR (Dubna); MON, RosAtom, RAS and RFBR (Russia); MESTD (Serbia); SEIDI and CPAN (Spain); Swiss Funding Agencies (Switzerland); MST (Taipei); ThEPCenter, IPST, STAR and NSTDA (Thailand); TUBITAK and TAEK (Turkey); NASU and SFFR (Ukraine); STFC (United Kingdom); DOE and NSF (USA).

Individuals have received support from the Marie-Curie programme and the European Research Council and EPLANET (European Union); the Leventis Foundation; the A.P. Sloan Foundation; the Alexander von Humboldt Foundation; the Belgian Federal Science Policy Office; the Fonds pour la Formation à la Recherche dans l'Industrie et dans l'Agriculture (FRIA-Belgium); the Agentschap voor Innovatie door Wetenschap en Technologie (IWT-Belgium); the Ministry of Education, Youth and Sports (MEYS) of the Czech Republic; the Council of Scientific and Industrial Research, India; the HOMING PLUS programme of the Foundation for Polish Science, cofinanced from European Union, Regional Development Fund; the OPUS programme of the National Science Centre (Poland); the Compagnia di San Paolo (Torino); MIUR project 20108T4XTM (Italy); the Thalis and Aristeia programmes cofinanced by EU-ESF and the Greek NSRF; the National Priorities Research Program by Qatar National Research Fund; the Rachadapisek Sompot Fund for Postdoctoral Fellowship, Chulalongkorn University (Thailand); and the Welch Foundation, contract C-1845.

References

[1] D. Krohn, T. Liu, J. Shelton, L.-T. Wang, A polarized view of the top asymmetry, Phys. Rev. D 84 (2011) 074034, http://dx.doi.org/10.1103/PhysRevD.84.074034, arXiv:1105.3743.

[2] W. Bernreuther, Z.-G. Si, Top quark spin correlations and polarization at the LHC: standard model predictions and effects of anomalous top chromo moments, Phys. Lett. B 725 (2013) 115, http://dx.doi.org/10.1016/j.physletb.2013.06.051, arXiv:1305.2066.

[3] T. Aaltonen, et al., CDF Collaboration, Measurement of $t\bar{t}$ spin correlation in $p\bar{p}$ collisions using the CDF II detector at the Tevatron, Phys. Rev. D 83 (2011) 031104, http://dx.doi.org/10.1103/PhysRevD.83.031104, arXiv:1012.3093.

[4] B. Abbott, et al., D0 Collaboration, Spin correlation in $t\bar{t}$ production from $p\bar{p}$ collisions at $\sqrt{s} = 1.8$ TeV, Phys. Rev. Lett. 85 (2000) 256, http://dx.doi.org/10.1103/PhysRevLett.85.256, arXiv:hep-ex/0002058.

[5] V.M. Abazov, et al., D0 Collaboration, Measurement of spin correlation in $t\bar{t}$ production using dilepton final states, Phys. Lett. B 702 (2011) 16, http://dx.doi.org/10.1016/j.physletb.2011.05.077, arXiv:1103.1871.

[6] V.M. Abazov, et al., D0 Collaboration, Measurement of spin correlation in $t\bar{t}$ production using a matrix element approach, Phys. Rev. Lett. 107 (2011) 032001, http://dx.doi.org/10.1103/PhysRevLett.107.032001, arXiv:1104.5194.

[7] V.M. Abazov, et al., D0 Collaboration, Evidence for spin correlation in $t\bar{t}$ production, Phys. Rev. Lett. 108 (2012) 032004, http://dx.doi.org/10.1103/PhysRevLett.108.032004, arXiv:1110.4194.

[8] ATLAS Collaboration, Observation of spin correlation in $t\bar{t}$ events from pp collisions at $\sqrt(s) = 7$ TeV using the ATLAS detector, Phys. Rev. Lett. 108 (2012) 212001, http://dx.doi.org/10.1103/PhysRevLett.108.212001, arXiv:1203.4081.

[9] ATLAS Collaboration, Measurement of spin correlation in top–antitop quark events and search for top squark pair production in pp collisions at $\sqrt{s} = 8$ TeV using the ATLAS detector, Phys. Rev. Lett. 114 (2015) 142001, http://dx.doi.org/10.1103/PhysRevLett.114.142001, arXiv:1412.4742.

[10] ATLAS Collaboration, Measurement of the correlations between the polar angles of leptons from top quark decays in the helicity basis at $\sqrt{s} = 7$ TeV using the ATLAS detector, Phys. Rev. D 93 (2016) 012002, http://dx.doi.org/10.1103/PhysRevD.93.012002, arXiv:1510.07478.

[11] ATLAS Collaboration, Measurements of spin correlation in top–antitop quark events from proton–proton collisions at $\sqrt{s} = 7$ TeV using the ATLAS detector, Phys. Rev. D 90 (2014) 112016, http://dx.doi.org/10.1103/PhysRevD.90.112016, arXiv:1407.4314.

[12] CMS Collaboration, The CMS experiment at the CERN LHC, J. Instrum. 3 (2008) S08004, http://dx.doi.org/10.1088/1748-0221/3/08/S08004.

[13] CMS Collaboration, Performance of CMS muon reconstruction in pp collision events at $\sqrt{s} = 7$ TeV, J. Instrum. 7 (2012) P10002, http://dx.doi.org/10.1088/1748-0221/7/10/P10002, arXiv:1206.4071.

[14] S. Frixione, B.R. Webber, Matching NLO QCD computations and parton shower simulations, J. High Energy Phys. 06 (2002) 029, http://dx.doi.org/10.1088/1126-6708/2002/06/029, arXiv:hep-ph/0204244.

[15] S. Frixione, F. Stoeckli, P. Torrielli, B.R. Webber, NLO QCD corrections in Herwig++ with MC@NLO, J. High Energy Phys. 01 (2011) 053, http://dx.doi.org/10.1007/JHEP01(2011)053, arXiv:1010.0568.

[16] H.-L. Lai, M. Guzzi, J. Huston, Z. Li, P.M. Nadolsky, J. Pumplin, C.-P. Yuan, New parton distributions for collider physics, Phys. Rev. D 82 (2010) 074024, http://dx.doi.org/10.1103/PhysRevD.82.074024, arXiv:1007.2241.

[17] J. Alwall, R. Frederix, S. Frixione, V. Hirschi, F. Maltoni, O. Mattelaer, H.-S. Shao, T. Stelzer, P. Torrielli, M. Zaro, The automated computation of tree-level and next-to-leading order differential cross sections, and their matching to parton shower simulations, J. High Energy Phys. 07 (2014) 079, http://dx.doi.org/10.1007/JHEP07(2014)079, arXiv:1405.0301.

[18] Z. Was, TAUOLA the library for tau lepton decay, and KKMC/KORALB/KORALZ/... status report, Nucl. Phys. B, Proc. Suppl. 98 (2001) 96, http://dx.doi.org/10.1016/S0920-5632(01)01200-2, arXiv:hep-ph/0011305.

[19] P. Nason, A new method for combining NLO QCD with shower Monte Carlo algorithms, J. High Energy Phys. 11 (2004) 040, http://dx.doi.org/10.1088/1126-6708/2004/11/040, arXiv:hep-ph/0409146.

[20] S. Frixione, P. Nason, C. Oleari, Matching NLO QCD computations with parton shower simulations: the POWHEG method, J. High Energy Phys. 11 (2007) 070, http://dx.doi.org/10.1088/1126-6708/2007/11/070, arXiv:0709.2092.

[21] S. Alioli, P. Nason, C. Oleari, E. Re, A general framework for implementing NLO calculations in shower Monte Carlo programs: the POWHEG BOX, J. High Energy Phys. 06 (2010) 043, http://dx.doi.org/10.1007/JHEP06(2010)043, arXiv:1002.2581.

[22] N. Davidson, G. Nanava, T. Przedzinski, E. Richter-Was, Z. Was, Universal interface of TAUOLA technical and physics documentation, Comput. Phys. Commun. 183 (2012) 821, http://dx.doi.org/10.1016/j.cpc.2011.12.009, arXiv:1002.0543.

[23] R. Field, Early LHC underlying event data – findings and surprises, in: Hadron Collider Physics, Proceedings, 22nd Conference, HCP 2010, Toronto, Canada, August 23–27, 2010, 2010, arXiv:1010.3558.

[24] J. Pumplin, D.R. Stump, J. Huston, H.-L. Lai, P. Nadolsky, W.-K. Tung, New generation of parton distributions with uncertainties from global QCD analysis, J. High Energy Phys. 07 (2002) 012, http://dx.doi.org/10.1088/1126-6708/2002/07/012, arXiv:hep-ph/0201195.

[25] S. Agostinelli, et al., GEANT4, GEANT4—a simulation toolkit, Nucl. Instrum. Methods Phys. Res., Sect. A, Accel. Spectrom. Detect. Assoc. Equip. 506 (2003) 250, http://dx.doi.org/10.1016/S0168-9002(03)01368-8.

[26] ATLAS, CDF, CMS and D0 Collaborations, First combination of Tevatron and LHC measurements of the top-quark mass, arXiv:1403.4427, 2014.

[27] M. Czakon, P. Fiedler, A. Mitov, The total top quark pair production cross-section at hadron colliders through $\mathcal{O}(\alpha_S^4)$, Phys. Rev. Lett. 110 (2013) 252004, http://dx.doi.org/10.1103/PhysRevLett.110.252004, arXiv:1303.6254.

[28] CMS Collaboration, Particle–flow event reconstruction in CMS and performance for jets, taus, and E_T^{miss}, CMS Physics Analysis Summary CMS-PAS-PFT-09-001, URL: http://cdsweb.cern.ch/record/1194487, 2009.

[29] CMS Collaboration, Commissioning of the particle-flow event reconstruction with the first LHC collisions recorded in the CMS detector, CMS Physics Analysis Summary CMS-PAS-PFT-10–001, URL: http://cdsweb.cern.ch/record/1247373, 2010.

[30] M. Cacciari, G.P. Salam, G. Soyez, The anti-k_t jet clustering algorithm, J. High Energy Phys. 04 (2008) 063, http://dx.doi.org/10.1088/1126-6708/2008/04/063, arXiv:0802.1189.

[31] M. Cacciari, G.P. Salam, G. Soyez, FastJet user manual, Eur. Phys. J. C 72 (2012) 1896, http://dx.doi.org/10.1140/epjc/s10052-012-1896-2, arXiv:1111.6097.

[32] CMS Collaboration, Identification and filtering of uncharacteristic noise in the CMS hadron calorimeter, J. Instrum. 5 (2010) T03014, http://dx.doi.org/10.1088/1748-0221/5/03/T03014, arXiv:0911.4881.

[33] CMS Collaboration, Identification of b-quark jets with the CMS experiment, J. Instrum. 8 (2013) P04013, http://dx.doi.org/10.1088/1748-0221/8/04/P04013, arXiv:1211.4462.

[34] B. Abbott, et al., D0 Collaboration, Direct measurement of the top quark mass by the D0 Collaboration, Phys. Rev. D 58 (1998) 052001, http://dx.doi.org/10.1103/PhysRevD.58.052001, arXiv:hep-ex/9801025.

[35] K. Kondo, Dynamical likelihood method for reconstruction of events with missing momentum. 1. Method and toy models, J. Phys. Soc. Jpn. 57 (1988) 4126, http://dx.doi.org/10.1143/JPSJ.57.4126.

[36] K. Kondo, Dynamical likelihood method for reconstruction of events with missing momentum. 2. Mass spectra for $2 \to 2$ processes, J. Phys. Soc. Jpn. 60 (1991) 836, http://dx.doi.org/10.1143/JPSJ.60.836.

[37] R.H. Dalitz, G.R. Goldstein, Analysis of top–antitop production and dilepton decay events and the top quark mass, Phys. Lett. B 287 (1992) 225, http://dx.doi.org/10.1016/0370-2693(92)91904-N.

[38] M. Abazov, et al., D0 Collaboration, A precision measurement of the mass of the top quark, Nature 429 (2004) 638, http://dx.doi.org/10.1038/nature02589, arXiv:hep-ex/0406031.

[39] P. Artoisenet, V. Lemaître, F. Maltoni, O. Mattelaer, Automation of the matrix element reweighting method, J. High Energy Phys. 12 (2010) 068, http://dx.doi.org/10.1007/JHEP12(2010)068, arXiv:1007.3300.

[40] R. Cousins, J. Mumford, J. Tucker, V. Valuev, Spin discrimination of new heavy resonances at the LHC, J. High Energy Phys. 11 (2005) 46, http://dx.doi.org/10.1088/1126-6708/2005/11/046.

[41] W. Verkerke, D. Kirkby, The RooFit toolkit for data modeling, arXiv:physics:data-an/0306116, 2003.

[42] F. James, M. Roos, Minuit: a system for function minimization and analysis of the parameter errors and correlations, Comput. Phys. Commun. 10 (1975) 343, http://dx.doi.org/10.1016/0010-4655(75)90039-9.

[43] CMS Collaboration, Determination of jet energy calibration and transverse momentum resolution in CMS, J. Instrum. 6 (2011) P11002, http://dx.doi.org/10.1088/1748-0221/6/11/P11002, arXiv:1107.4277.

[44] CMS Collaboration, 8 TeV jet energy corrections and uncertainties based on 19.8 fb^{-1} of data in CMS, CMS Detector Performance Note CMS-DP-2013-033. URL: https://cds.cern.ch/record/1627305, 2013.

[45] S. Alekhin, et al., The PDF4LHC Working Group interim report, arXiv:1101.0536, 2011.

[46] M. Botje, J. Butterworth, A. Cooper-Sarkar, A. de Roeck, J. Feltesse, S. Forte, A. Glazov, J. Huston, R. McNulty, T. Sjöstrand, R.S. Thorne, The PDF4LHC Working Group interim recommendations, arXiv:1101.0538, 2011.

[47] CMS Collaboration, Measurement of differential top-quark pair production cross sections in pp collisions at $\sqrt{s} = 7$ TeV, Eur. Phys. J. C 73 (2013) 2339, http://dx.doi.org/10.1140/epjc/s10052-013-2339-4, arXiv:1211.2220 [hep-ph].

[48] CMS Collaboration, Measurement of the differential cross section for top quark pair production in pp collisions at $\sqrt{s} = 8$ TeV, Eur. Phys. J. C 75 (2015) 542, http://dx.doi.org/10.1140/epjc/s10052-015-3709-x, arXiv:1505.04480.

[49] G. Antchev, et al., TOTEM Collaboration, First measurement of the total proton–proton cross section at the LHC energy of $\sqrt{s} = 7$ TeV, Europhys. Lett. 96 (2011) 21002, http://dx.doi.org/10.1209/0295-5075/96/21002, arXiv:1110.1395.

[50] CMS Collaboration, Performance of b tagging at $\sqrt{s} = 8$ TeV in multijet, $t\bar{t}$ and boosted topology events, CMS Physics Analysis Summary CMS-PAS-BTV-13-001, URL: https://cds.cern.ch/record/1581306, 2013.

[51] W. Bernreuther, A. Brandenburg, Z.G. Si, P. Uwer, Top quark pair production and decay at hadron colliders, Nucl. Phys. B 690 (2004) 81, http://dx.doi.org/10.1016/j.nuclphysb.2004.04.019, arXiv:hep-ph/0403035.

[52] W. Bernreuther, D. Heisler, Z.-G. Si, A set of top quark spin correlation and polarization observables for the LHC: standard model predictions and new physics contributions, J. High Energy Phys. 12 (2015) 026, http://dx.doi.org/10.1007/JHEP12(2015)026, arXiv:1508.05271.

CMS Collaboration

V. Khachatryan, A.M. Sirunyan, A. Tumasyan

Yerevan Physics Institute, Yerevan, Armenia

W. Adam, E. Asilar, T. Bergauer, J. Brandstetter, E. Brondolin, M. Dragicevic, J. Erö, M. Flechl, M. Friedl, R. Frühwirth [1], V.M. Ghete, C. Hartl, N. Hörmann, J. Hrubec, M. Jeitler [1], V. Knünz, A. König, M. Krammer [1], I. Krätschmer, D. Liko, T. Matsushita, I. Mikulec, D. Rabady [2], B. Rahbaran, H. Rohringer, J. Schieck [1], R. Schöfbeck, J. Strauss, W. Treberer-Treberspurg, W. Waltenberger, C.-E. Wulz [1]

Institut für Hochenergiephysik der OeAW, Wien, Austria

V. Mossolov, N. Shumeiko, J. Suarez Gonzalez

National Centre for Particle and High Energy Physics, Minsk, Belarus

S. Alderweireldt, T. Cornelis, E.A. De Wolf, X. Janssen, A. Knutsson, J. Lauwers, S. Luyckx, R. Rougny, M. Van De Klundert, H. Van Haevermaet, P. Van Mechelen, N. Van Remortel, A. Van Spilbeeck

Universiteit Antwerpen, Antwerpen, Belgium

S. Abu Zeid, F. Blekman, J. D'Hondt, N. Daci, I. De Bruyn, K. Deroover, N. Heracleous, J. Keaveney, S. Lowette, L. Moreels, A. Olbrechts, Q. Python, D. Strom, S. Tavernier, W. Van Doninck, P. Van Mulders, G.P. Van Onsem, I. Van Parijs

Vrije Universiteit Brussel, Brussel, Belgium

P. Barria, H. Brun, C. Caillol, B. Clerbaux, G. De Lentdecker, G. Fasanella, L. Favart, A. Grebenyuk, G. Karapostoli, T. Lenzi, A. Léonard, T. Maerschalk, A. Marinov, L. Perniè, A. Randle-conde, T. Reis, T. Seva, C. Vander Velde, P. Vanlaer, R. Yonamine, F. Zenoni, F. Zhang [3]

Université Libre de Bruxelles, Bruxelles, Belgium

K. Beernaert, L. Benucci, A. Cimmino, S. Crucy, D. Dobur, A. Fagot, G. Garcia, M. Gul, J. Mccartin, A.A. Ocampo Rios, D. Poyraz, D. Ryckbosch, S. Salva, M. Sigamani, N. Strobbe, M. Tytgat, W. Van Driessche, E. Yazgan, N. Zaganidis

Ghent University, Ghent, Belgium

S. Basegmez, C. Beluffi [4], O. Bondu, S. Brochet, G. Bruno, A. Caudron, L. Ceard, G.G. Da Silveira, C. Delaere, D. Favart, L. Forthomme, A. Giammanco [5], J. Hollar, A. Jafari, P. Jez, M. Komm, V. Lemaitre, A. Mertens, C. Nuttens, L. Perrini, A. Pin, K. Piotrzkowski, A. Popov [6], L. Quertenmont, M. Selvaggi, M. Vidal Marono

Université Catholique de Louvain, Louvain-la-Neuve, Belgium

N. Beliy, G.H. Hammad

Université de Mons, Mons, Belgium

W.L. Aldá Júnior, G.A. Alves, L. Brito, M. Correa Martins Junior, M. Hamer, C. Hensel, C. Mora Herrera, A. Moraes, M.E. Pol, P. Rebello Teles

Centro Brasileiro de Pesquisas Fisicas, Rio de Janeiro, Brazil

E. Belchior Batista Das Chagas, W. Carvalho, J. Chinellato [7], A. Custódio, E.M. Da Costa, D. De Jesus Damiao, C. De Oliveira Martins, S. Fonseca De Souza, L.M. Huertas Guativa, H. Malbouisson, D. Matos Figueiredo, L. Mundim, H. Nogima, W.L. Prado Da Silva, A. Santoro, A. Sznajder, E.J. Tonelli Manganote [7], A. Vilela Pereira

Universidade do Estado do Rio de Janeiro, Rio de Janeiro, Brazil

S. Ahuja [a], C.A. Bernardes [b], A. De Souza Santos [b], S. Dogra [a], T.R. Fernandez Perez Tomei [a], E.M. Gregores [b], P.G. Mercadante [b], C.S. Moon [a,8], S.F. Novaes [a], Sandra S. Padula [a], D. Romero Abad, J.C. Ruiz Vargas

[a] *Universidade Estadual Paulista, São Paulo, Brazil*
[b] *Universidade Federal do ABC, São Paulo, Brazil*

A. Aleksandrov, R. Hadjiiska, P. Iaydjiev, M. Rodozov, S. Stoykova, G. Sultanov, M. Vutova

Institute for Nuclear Research and Nuclear Energy, Sofia, Bulgaria

A. Dimitrov, I. Glushkov, L. Litov, B. Pavlov, P. Petkov

University of Sofia, Sofia, Bulgaria

M. Ahmad, J.G. Bian, G.M. Chen, H.S. Chen, M. Chen, T. Cheng, R. Du, C.H. Jiang, R. Plestina [9], F. Romeo, S.M. Shaheen, J. Tao, C. Wang, Z. Wang, H. Zhang

Institute of High Energy Physics, Beijing, China

C. Asawatangtrakuldee, Y. Ban, Q. Li, S. Liu, Y. Mao, S.J. Qian, D. Wang, Z. Xu, W. Zou

State Key Laboratory of Nuclear Physics and Technology, Peking University, Beijing, China

C. Avila, A. Cabrera, L.F. Chaparro Sierra, C. Florez, J.P. Gomez, B. Gomez Moreno, J.C. Sanabria

Universidad de Los Andes, Bogota, Colombia

N. Godinovic, D. Lelas, I. Puljak, P.M. Ribeiro Cipriano

University of Split, Faculty of Electrical Engineering, Mechanical Engineering and Naval Architecture, Split, Croatia

Z. Antunovic, M. Kovac

University of Split, Faculty of Science, Split, Croatia

V. Brigljevic, K. Kadija, J. Luetic, S. Micanovic, L. Sudic

Institute Rudjer Boskovic, Zagreb, Croatia

A. Attikis, G. Mavromanolakis, J. Mousa, C. Nicolaou, F. Ptochos, P.A. Razis, H. Rykaczewski

University of Cyprus, Nicosia, Cyprus

M. Bodlak, M. Finger [10], M. Finger Jr. [10]

Charles University, Prague, Czech Republic

M. El Sawy [11,12], E. El-khateeb [13], T. Elkafrawy [13], A. Mohamed [14], E. Salama [12,13]

Academy of Scientific Research and Technology of the Arab Republic of Egypt, Egyptian Network of High Energy Physics, Cairo, Egypt

B. Calpas, M. Kadastik, M. Murumaa, M. Raidal, A. Tiko, C. Veelken

National Institute of Chemical Physics and Biophysics, Tallinn, Estonia

P. Eerola, J. Pekkanen, M. Voutilainen

Department of Physics, University of Helsinki, Helsinki, Finland

J. Härkönen, V. Karimäki, R. Kinnunen, T. Lampén, K. Lassila-Perini, S. Lehti, T. Lindén, P. Luukka, T. Mäenpää, T. Peltola, E. Tuominen, J. Tuominiemi, E. Tuovinen, L. Wendland

Helsinki Institute of Physics, Helsinki, Finland

J. Talvitie, T. Tuuva

Lappeenranta University of Technology, Lappeenranta, Finland

M. Besancon, F. Couderc, M. Dejardin, D. Denegri, B. Fabbro, J.L. Faure, C. Favaro, F. Ferri, S. Ganjour, A. Givernaud, P. Gras, G. Hamel de Monchenault, P. Jarry, E. Locci, M. Machet, J. Malcles, J. Rander, A. Rosowsky, M. Titov, A. Zghiche

DSM/IRFU, CEA/Saclay, Gif-sur-Yvette, France

I. Antropov, S. Baffioni, F. Beaudette, P. Busson, L. Cadamuro, E. Chapon, C. Charlot, T. Dahms, O. Davignon, N. Filipovic, A. Florent, R. Granier de Cassagnac, S. Lisniak, L. Mastrolorenzo, P. Miné, I.N. Naranjo, M. Nguyen, C. Ochando, G. Ortona, P. Paganini, P. Pigard, S. Regnard, R. Salerno, J.B. Sauvan, Y. Sirois, T. Strebler, Y. Yilmaz, A. Zabi

Laboratoire Leprince-Ringuet, Ecole Polytechnique, IN2P3-CNRS, Palaiseau, France

J.-L. Agram [15], J. Andrea, A. Aubin, D. Bloch, J.-M. Brom, M. Buttignol, E.C. Chabert, N. Chanon, C. Collard, E. Conte [15], X. Coubez, J.-C. Fontaine [15], D. Gelé, U. Goerlach, C. Goetzmann, A.-C. Le Bihan, J.A. Merlin [2], K. Skovpen, P. Van Hove

Institut Pluridisciplinaire Hubert Curien, Université de Strasbourg, Université de Haute Alsace Mulhouse, CNRS/IN2P3, Strasbourg, France

S. Gadrat

Centre de Calcul de l'Institut National de Physique Nucleaire et de Physique des Particules, CNRS/IN2P3, Villeurbanne, France

S. Beauceron, C. Bernet, G. Boudoul, E. Bouvier, C.A. Carrillo Montoya, R. Chierici, D. Contardo, B. Courbon, P. Depasse, H. El Mamouni, J. Fan, J. Fay, S. Gascon, M. Gouzevitch, B. Ille, F. Lagarde, I.B. Laktineh, M. Lethuillier, L. Mirabito, A.L. Pequegnot, S. Perries, J.D. Ruiz Alvarez, D. Sabes, L. Sgandurra, V. Sordini, M. Vander Donckt, P. Verdier, S. Viret

Université de Lyon, Université Claude Bernard Lyon 1, CNRS-IN2P3, Institut de Physique Nucléaire de Lyon, Villeurbanne, France

T. Toriashvili [16]

Georgian Technical University, Tbilisi, Georgia

D. Lomidze

Tbilisi State University, Tbilisi, Georgia

C. Autermann, S. Beranek, M. Edelhoff, L. Feld, A. Heister, M.K. Kiesel, K. Klein, M. Lipinski, A. Ostapchuk, M. Preuten, F. Raupach, S. Schael, J.F. Schulte, T. Verlage, H. Weber, B. Wittmer, V. Zhukov [6]

RWTH Aachen University, I. Physikalisches Institut, Aachen, Germany

M. Ata, M. Brodski, E. Dietz-Laursonn, D. Duchardt, M. Endres, M. Erdmann, S. Erdweg, T. Esch, R. Fischer, A. Güth, T. Hebbeker, C. Heidemann, K. Hoepfner, D. Klingebiel, S. Knutzen, P. Kreuzer, M. Merschmeyer, A. Meyer, P. Millet, M. Olschewski, K. Padeken, P. Papacz, T. Pook, M. Radziej, H. Reithler, M. Rieger, F. Scheuch, L. Sonnenschein, D. Teyssier, S. Thüer

RWTH Aachen University, III. Physikalisches Institut A, Aachen, Germany

V. Cherepanov, Y. Erdogan, G. Flügge, H. Geenen, M. Geisler, F. Hoehle, B. Kargoll, T. Kress, Y. Kuessel, A. Künsken, J. Lingemann [2], A. Nehrkorn, A. Nowack, I.M. Nugent, C. Pistone, O. Pooth, A. Stahl

RWTH Aachen University, III. Physikalisches Institut B, Aachen, Germany

M. Aldaya Martin, I. Asin, N. Bartosik, O. Behnke, U. Behrens, A.J. Bell, K. Borras, A. Burgmeier, A. Cakir, L. Calligaris, A. Campbell, S. Choudhury, F. Costanza, C. Diez Pardos, G. Dolinska, S. Dooling, T. Dorland,

G. Eckerlin, D. Eckstein, T. Eichhorn, G. Flucke, E. Gallo [17], J. Garay Garcia, A. Geiser, A. Gizhko, P. Gunnellini, J. Hauk, M. Hempel [18], H. Jung, A. Kalogeropoulos, O. Karacheban [18], M. Kasemann, P. Katsas, J. Kieseler, C. Kleinwort, I. Korol, W. Lange, J. Leonard, K. Lipka, A. Lobanov, W. Lohmann [18], R. Mankel, I. Marfin [18], I.-A. Melzer-Pellmann, A.B. Meyer, G. Mittag, J. Mnich, A. Mussgiller, S. Naumann-Emme, A. Nayak, E. Ntomari, H. Perrey, D. Pitzl, R. Placakyte, A. Raspereza, B. Roland, M.Ö. Sahin, P. Saxena, T. Schoerner-Sadenius, M. Schröder, C. Seitz, S. Spannagel, K.D. Trippkewitz, R. Walsh, C. Wissing

Deutsches Elektronen-Synchrotron, Hamburg, Germany

V. Blobel, M. Centis Vignali, A.R. Draeger, J. Erfle, E. Garutti, K. Goebel, D. Gonzalez, M. Görner, J. Haller, M. Hoffmann, R.S. Höing, A. Junkes, R. Klanner, R. Kogler, T. Lapsien, T. Lenz, I. Marchesini, D. Marconi, M. Meyer, D. Nowatschin, J. Ott, F. Pantaleo [2], T. Peiffer, A. Perieanu, N. Pietsch, J. Poehlsen, D. Rathjens, C. Sander, H. Schettler, P. Schleper, E. Schlieckau, A. Schmidt, J. Schwandt, M. Seidel, V. Sola, H. Stadie, G. Steinbrück, H. Tholen, D. Troendle, E. Usai, L. Vanelderen, A. Vanhoefer, B. Vormwald

University of Hamburg, Hamburg, Germany

M. Akbiyik, C. Barth, C. Baus, J. Berger, C. Böser, E. Butz, T. Chwalek, F. Colombo, W. De Boer, A. Descroix, A. Dierlamm, S. Fink, F. Frensch, M. Giffels, A. Gilbert, F. Hartmann [2], S.M. Heindl, U. Husemann, I. Katkov [6], A. Kornmayer [2], P. Lobelle Pardo, B. Maier, H. Mildner, M.U. Mozer, T. Müller, Th. Müller, M. Plagge, G. Quast, K. Rabbertz, S. Röcker, F. Roscher, H.J. Simonis, F.M. Stober, R. Ulrich, J. Wagner-Kuhr, S. Wayand, M. Weber, T. Weiler, C. Wöhrmann, R. Wolf

Institut für Experimentelle Kernphysik, Karlsruhe, Germany

G. Anagnostou, G. Daskalakis, T. Geralis, V.A. Giakoumopoulou, A. Kyriakis, D. Loukas, A. Psallidas, I. Topsis-Giotis

Institute of Nuclear and Particle Physics (INPP), NCSR Demokritos, Aghia Paraskevi, Greece

A. Agapitos, S. Kesisoglou, A. Panagiotou, N. Saoulidou, E. Tziaferi

University of Athens, Athens, Greece

I. Evangelou, G. Flouris, C. Foudas, P. Kokkas, N. Loukas, N. Manthos, I. Papadopoulos, E. Paradas, J. Strologas

University of Ioánnina, Ioánnina, Greece

G. Bencze, C. Hajdu, A. Hazi, P. Hidas, D. Horvath [19], F. Sikler, V. Veszpremi, G. Vesztergombi [20], A.J. Zsigmond

Wigner Research Centre for Physics, Budapest, Hungary

N. Beni, S. Czellar, J. Karancsi [21], J. Molnar, Z. Szillasi

Institute of Nuclear Research ATOMKI, Debrecen, Hungary

M. Bartók [22], A. Makovec, P. Raics, Z.L. Trocsanyi, B. Ujvari

University of Debrecen, Debrecen, Hungary

P. Mal, K. Mandal, D.K. Sahoo, N. Sahoo, S.K. Swain

National Institute of Science Education and Research, Bhubaneswar, India

S. Bansal, S.B. Beri, V. Bhatnagar, R. Chawla, R. Gupta, U. Bhawandeep, A.K. Kalsi, A. Kaur, M. Kaur, R. Kumar, A. Mehta, M. Mittal, J.B. Singh, G. Walia

Panjab University, Chandigarh, India

Ashok Kumar, A. Bhardwaj, B.C. Choudhary, R.B. Garg, A. Kumar, S. Malhotra, M. Naimuddin, N. Nishu, K. Ranjan, R. Sharma, V. Sharma

University of Delhi, Delhi, India

S. Bhattacharya, K. Chatterjee, S. Dey, S. Dutta, Sa. Jain, N. Majumdar, A. Modak, K. Mondal, S. Mukherjee, S. Mukhopadhyay, A. Roy, D. Roy, S. Roy Chowdhury, S. Sarkar, M. Sharan

Saha Institute of Nuclear Physics, Kolkata, India

A. Abdulsalam, R. Chudasama, D. Dutta, V. Jha, V. Kumar, A.K. Mohanty [2], L.M. Pant, P. Shukla, A. Topkar

Bhabha Atomic Research Centre, Mumbai, India

T. Aziz, S. Banerjee, S. Bhowmik [23], R.M. Chatterjee, R.K. Dewanjee, S. Dugad, S. Ganguly, S. Ghosh, M. Guchait, A. Gurtu [24], G. Kole, S. Kumar, B. Mahakud, M. Maity [23], G. Majumder, K. Mazumdar, S. Mitra, G.B. Mohanty, B. Parida, T. Sarkar [23], K. Sudhakar, N. Sur, B. Sutar, N. Wickramage [25]

Tata Institute of Fundamental Research, Mumbai, India

S. Chauhan, S. Dube, S. Sharma

Indian Institute of Science Education and Research (IISER), Pune, India

H. Bakhshiansohi, H. Behnamian, S.M. Etesami [26], A. Fahim [27], R. Goldouzian, M. Khakzad, M. Mohammadi Najafabadi, M. Naseri, S. Paktinat Mehdiabadi, F. Rezaei Hosseinabadi, B. Safarzadeh [28], M. Zeinali

Institute for Research in Fundamental Sciences (IPM), Tehran, Iran

M. Felcini, M. Grunewald

University College Dublin, Dublin, Ireland

M. Abbrescia [a,b], C. Calabria [a,b], C. Caputo [a,b], A. Colaleo [a], D. Creanza [a,c], L. Cristella [a,b], N. De Filippis [a,c], M. De Palma [a,b], L. Fiore [a], G. Iaselli [a,c], G. Maggi [a,c], M. Maggi [a], G. Miniello [a,b], S. My [a,c], S. Nuzzo [a,b], A. Pompili [a,b], G. Pugliese [a,c], R. Radogna [a,b], A. Ranieri [a], G. Selvaggi [a,b], L. Silvestris [a,2], R. Venditti [a,b], P. Verwilligen [a]

[a] *INFN Sezione di Bari, Bari, Italy*
[b] *Università di Bari, Bari, Italy*
[c] *Politecnico di Bari, Bari, Italy*

G. Abbiendi [a], C. Battilana [2], A.C. Benvenuti [a], D. Bonacorsi [a,b], S. Braibant-Giacomelli [a,b], L. Brigliadori [a,b], R. Campanini [a,b], P. Capiluppi [a,b], A. Castro [a,b], F.R. Cavallo [a], S.S. Chhibra [a,b], G. Codispoti [a,b], M. Cuffiani [a,b], G.M. Dallavalle [a], F. Fabbri [a], A. Fanfani [a,b], D. Fasanella [a,b], P. Giacomelli [a], C. Grandi [a], L. Guiducci [a,b], S. Marcellini [a], G. Masetti [a], A. Montanari [a], F.L. Navarria [a,b], A. Perrotta [a], A.M. Rossi [a,b], T. Rovelli [a,b], G.P. Siroli [a,b], N. Tosi [a,b], R. Travaglini [a,b]

[a] *INFN Sezione di Bologna, Bologna, Italy*
[b] *Università di Bologna, Bologna, Italy*

G. Cappello [a], M. Chiorboli [a,b], S. Costa [a,b], F. Giordano [a,b], R. Potenza [a,b], A. Tricomi [a,b], C. Tuve [a,b]

[a] *INFN Sezione di Catania, Catania, Italy*
[b] *Università di Catania, Catania, Italy*

G. Barbagli [a], V. Ciulli [a,b], C. Civinini [a], R. D'Alessandro [a,b], E. Focardi [a,b], S. Gonzi [a,b], V. Gori [a,b], P. Lenzi [a,b], M. Meschini [a], S. Paoletti [a], G. Sguazzoni [a], A. Tropiano [a,b], L. Viliani [a,b]

[a] *INFN Sezione di Firenze, Firenze, Italy*
[b] *Università di Firenze, Firenze, Italy*

L. Benussi, S. Bianco, F. Fabbri, D. Piccolo, F. Primavera

INFN Laboratori Nazionali di Frascati, Frascati, Italy

V. Calvelli [a,b], F. Ferro [a], M. Lo Vetere [a,b], M.R. Monge [a,b], E. Robutti [a], S. Tosi [a,b]

[a] *INFN Sezione di Genova, Genova, Italy*
[b] *Università di Genova, Genova, Italy*

L. Brianza, M.E. Dinardo [a,b], S. Fiorendi [a,b], S. Gennai [a], R. Gerosa [a,b], A. Ghezzi [a,b], P. Govoni [a,b], S. Malvezzi [a], R.A. Manzoni [a,b], B. Marzocchi [a,b,2], D. Menasce [a], L. Moroni [a], M. Paganoni [a,b], D. Pedrini [a], S. Ragazzi [a,b], N. Redaelli [a], T. Tabarelli de Fatis [a,b]

[a] *INFN Sezione di Milano-Bicocca, Milano, Italy*
[b] *Università di Milano-Bicocca, Milano, Italy*

S. Buontempo [a], N. Cavallo [a,c], S. Di Guida [a,d,2], M. Esposito [a,b], F. Fabozzi [a,c], A.O.M. Iorio [a,b], G. Lanza [a], L. Lista [a], S. Meola [a,d,2], M. Merola [a], P. Paolucci [a,2], C. Sciacca [a,b], F. Thyssen

[a] *INFN Sezione di Napoli, Napoli, Italy*
[b] *Università di Napoli 'Federico II', Napoli, Italy*
[c] *Università della Basilicata, Potenza, Italy*
[d] *Università G. Marconi, Roma, Italy*

P. Azzi [a,2], N. Bacchetta [a], L. Benato [a,b], D. Bisello [a,b], A. Boletti [a,b], A. Branca [a,b], R. Carlin [a,b], P. Checchia [a], M. Dall'Osso [a,b,2], T. Dorigo [a], U. Dosselli [a], F. Gasparini [a,b], U. Gasparini [a,b], A. Gozzelino [a], K. Kanishchev [a,c], S. Lacaprara [a], M. Margoni [a,b], A.T. Meneguzzo [a,b], J. Pazzini [a,b], M. Pegoraro [a], N. Pozzobon [a,b], P. Ronchese [a,b], F. Simonetto [a,b], E. Torassa [a], M. Tosi [a,b], M. Zanetti, P. Zotto [a,b], A. Zucchetta [a,b,2], G. Zumerle [a,b]

[a] *INFN Sezione di Padova, Padova, Italy*
[b] *Università di Padova, Padova, Italy*
[c] *Università di Trento, Trento, Italy*

A. Braghieri [a], A. Magnani [a], P. Montagna [a,b], S.P. Ratti [a,b], V. Re [a], C. Riccardi [a,b], P. Salvini [a], I. Vai [a], P. Vitulo [a,b]

[a] *INFN Sezione di Pavia, Pavia, Italy*
[b] *Università di Pavia, Pavia, Italy*

L. Alunni Solestizi [a,b], M. Biasini [a,b], G.M. Bilei [a], D. Ciangottini [a,b,2], L. Fanò [a,b], P. Lariccia [a,b], G. Mantovani [a,b], M. Menichelli [a], A. Saha [a], A. Santocchia [a,b], A. Spiezia [a,b]

[a] *INFN Sezione di Perugia, Perugia, Italy*
[b] *Università di Perugia, Perugia, Italy*

K. Androsov [a,29], P. Azzurri [a], G. Bagliesi [a], J. Bernardini [a], T. Boccali [a], G. Broccolo [a,c], R. Castaldi [a], M.A. Ciocci [a,29], R. Dell'Orso [a], S. Donato [a,c,2], G. Fedi, L. Foà [a,c,†], A. Giassi [a], M.T. Grippo [a,29], F. Ligabue [a,c], T. Lomtadze [a], L. Martini [a,b], A. Messineo [a,b], F. Palla [a], A. Rizzi [a,b], A. Savoy-Navarro [a,30], A.T. Serban [a], P. Spagnolo [a], P. Squillacioti [a,29], R. Tenchini [a], G. Tonelli [a,b], A. Venturi [a], P.G. Verdini [a]

[a] *INFN Sezione di Pisa, Pisa, Italy*
[b] *Università di Pisa, Pisa, Italy*
[c] *Scuola Normale Superiore di Pisa, Pisa, Italy*

L. Barone [a,b], F. Cavallari [a], G. D'imperio [a,b,2], D. Del Re [a,b], M. Diemoz [a], S. Gelli [a,b], C. Jorda [a], E. Longo [a,b], F. Margaroli [a,b], P. Meridiani [a], G. Organtini [a,b], R. Paramatti [a], F. Preiato [a,b], S. Rahatlou [a,b], C. Rovelli [a], F. Santanastasio [a,b], P. Traczyk [a,b,2]

[a] *INFN Sezione di Roma, Roma, Italy*
[b] *Università di Roma, Roma, Italy*

N. Amapane [a,b], R. Arcidiacono [a,c,2], S. Argiro [a,b], M. Arneodo [a,c], R. Bellan [a,b], C. Biino [a], N. Cartiglia [a], M. Costa [a,b], R. Covarelli [a,b], A. Degano [a,b], G. Dellacasa [a], N. Demaria [a], L. Finco [a,b,2], C. Mariotti [a], S. Maselli [a], E. Migliore [a,b], V. Monaco [a,b], E. Monteil [a,b], M. Musich [a], M.M. Obertino [a,b], L. Pacher [a,b], N. Pastrone [a], M. Pelliccioni [a], G.L. Pinna Angioni [a,b], F. Ravera [a,b], A. Romero [a,b], M. Ruspa [a,c], R. Sacchi [a,b], A. Solano [a,b], A. Staiano [a], U. Tamponi [a]

[a] *INFN Sezione di Torino, Torino, Italy*
[b] *Università di Torino, Torino, Italy*
[c] *Università del Piemonte Orientale, Novara, Italy*

S. Belforte [a], V. Candelise [a,b,2], M. Casarsa [a], F. Cossutti [a], G. Della Ricca [a,b], B. Gobbo [a], C. La Licata [a,b], M. Marone [a,b], A. Schizzi [a,b], A. Zanetti [a]

[a] *INFN Sezione di Trieste, Trieste, Italy*
[b] *Università di Trieste, Trieste, Italy*

A. Kropivnitskaya, S.K. Nam

Kangwon National University, Chunchon, Republic of Korea

D.H. Kim, G.N. Kim, M.S. Kim, D.J. Kong, S. Lee, Y.D. Oh, A. Sakharov, D.C. Son

Kyungpook National University, Daegu, Republic of Korea

J.A. Brochero Cifuentes, H. Kim, T.J. Kim, M.S. Ryu

Chonbuk National University, Jeonju, Republic of Korea

S. Song

Chonnam National University, Institute for Universe and Elementary Particles, Kwangju, Republic of Korea

S. Choi, Y. Go, D. Gyun, B. Hong, M. Jo, H. Kim, Y. Kim, B. Lee, K. Lee, K.S. Lee, S. Lee, S.K. Park, Y. Roh

Korea University, Seoul, Republic of Korea

H.D. Yoo

Seoul National University, Seoul, Republic of Korea

M. Choi, H. Kim, J.H. Kim, J.S.H. Lee, I.C. Park, G. Ryu

University of Seoul, Seoul, Republic of Korea

Y. Choi, J. Goh, D. Kim, E. Kwon, J. Lee, I. Yu

Sungkyunkwan University, Suwon, Republic of Korea

A. Juodagalvis, J. Vaitkus

Vilnius University, Vilnius, Lithuania

I. Ahmed, Z.A. Ibrahim, J.R. Komaragiri, M.A.B. Md Ali [31], F. Mohamad Idris [32], W.A.T. Wan Abdullah, M.N. Yusli

National Centre for Particle Physics, Universiti Malaya, Kuala Lumpur, Malaysia

E. Casimiro Linares, H. Castilla-Valdez, E. De La Cruz-Burelo, I. Heredia-de La Cruz [33], A. Hernandez-Almada, R. Lopez-Fernandez, A. Sanchez-Hernandez

Centro de Investigacion y de Estudios Avanzados del IPN, Mexico City, Mexico

S. Carrillo Moreno, F. Vazquez Valencia

Universidad Iberoamericana, Mexico City, Mexico

I. Pedraza, H.A. Salazar Ibarguen

Benemerita Universidad Autonoma de Puebla, Puebla, Mexico

A. Morelos Pineda

Universidad Autónoma de San Luis Potosí, San Luis Potosí, Mexico

D. Krofcheck

University of Auckland, Auckland, New Zealand

P.H. Butler

University of Canterbury, Christchurch, New Zealand

A. Ahmad, M. Ahmad, Q. Hassan, H.R. Hoorani, W.A. Khan, T. Khurshid, M. Shoaib

National Centre for Physics, Quaid-I-Azam University, Islamabad, Pakistan

H. Bialkowska, M. Bluj, B. Boimska, T. Frueboes, M. Górski, M. Kazana, K. Nawrocki, K. Romanowska-Rybinska, M. Szleper, P. Zalewski

National Centre for Nuclear Research, Swierk, Poland

G. Brona, K. Bunkowski, A. Byszuk [34], K. Doroba, A. Kalinowski, M. Konecki, J. Krolikowski, M. Misiura, M. Olszewski, M. Walczak

Institute of Experimental Physics, Faculty of Physics, University of Warsaw, Warsaw, Poland

P. Bargassa, C. Beirão Da Cruz E Silva, A. Di Francesco, P. Faccioli, P.G. Ferreira Parracho, M. Gallinaro, N. Leonardo, L. Lloret Iglesias, F. Nguyen, J. Rodrigues Antunes, J. Seixas, O. Toldaiev, D. Vadruccio, J. Varela, P. Vischia

Laboratório de Instrumentação e Física Experimental de Partículas, Lisboa, Portugal

S. Afanasiev, P. Bunin, M. Gavrilenko, I. Golutvin, I. Gorbunov, A. Kamenev, V. Karjavin, V. Konoplyanikov, A. Lanev, A. Malakhov, V. Matveev [35], P. Moisenz, V. Palichik, V. Perelygin, S. Shmatov, S. Shulha, N. Skatchkov, V. Smirnov, A. Zarubin

Joint Institute for Nuclear Research, Dubna, Russia

V. Golovtsov, Y. Ivanov, V. Kim [36], E. Kuznetsova, P. Levchenko, V. Murzin, V. Oreshkin, I. Smirnov, V. Sulimov, L. Uvarov, S. Vavilov, A. Vorobyev

Petersburg Nuclear Physics Institute, Gatchina (St. Petersburg), Russia

Yu. Andreev, A. Dermenev, S. Gninenko, N. Golubev, A. Karneyeu, M. Kirsanov, N. Krasnikov, A. Pashenkov, D. Tlisov, A. Toropin

Institute for Nuclear Research, Moscow, Russia

V. Epshteyn, V. Gavrilov, N. Lychkovskaya, V. Popov, I. Pozdnyakov, G. Safronov, A. Spiridonov, E. Vlasov, A. Zhokin

Institute for Theoretical and Experimental Physics, Moscow, Russia

A. Bylinkin

National Research Nuclear University 'Moscow Engineering Physics Institute' (MEPhI), Moscow, Russia

V. Andreev, M. Azarkin [37], I. Dremin [37], M. Kirakosyan, A. Leonidov [37], G. Mesyats, S.V. Rusakov, A. Vinogradov

P.N. Lebedev Physical Institute, Moscow, Russia

A. Baskakov, A. Belyaev, E. Boos, V. Bunichev, M. Dubinin [38], L. Dudko, A. Ershov, V. Klyukhin, N. Korneeva, I. Lokhtin, I. Myagkov, S. Obraztsov, M. Perfilov, S. Petrushanko, V. Savrin

Skobeltsyn Institute of Nuclear Physics, Lomonosov Moscow State University, Moscow, Russia

I. Azhgirey, I. Bayshev, S. Bitioukov, V. Kachanov, A. Kalinin, D. Konstantinov, V. Krychkine, V. Petrov, R. Ryutin, A. Sobol, L. Tourtchanovitch, S. Troshin, N. Tyurin, A. Uzunian, A. Volkov

State Research Center of Russian Federation, Institute for High Energy Physics, Protvino, Russia

P. Adzic [39], M. Ekmedzic, J. Milosevic, V. Rekovic

University of Belgrade, Faculty of Physics and Vinca Institute of Nuclear Sciences, Belgrade, Serbia

J. Alcaraz Maestre, E. Calvo, M. Cerrada, M. Chamizo Llatas, N. Colino, B. De La Cruz, A. Delgado Peris, D. Domínguez Vázquez, A. Escalante Del Valle, C. Fernandez Bedoya, J.P. Fernández Ramos, J. Flix, M.C. Fouz, P. Garcia-Abia, O. Gonzalez Lopez, S. Goy Lopez, J.M. Hernandez, M.I. Josa, E. Navarro De Martino, A. Pérez-Calero Yzquierdo, J. Puerta Pelayo, A. Quintario Olmeda, I. Redondo, L. Romero, M.S. Soares

Centro de Investigaciones Energéticas Medioambientales y Tecnológicas (CIEMAT), Madrid, Spain

C. Albajar, J.F. de Trocóniz, M. Missiroli, D. Moran

Universidad Autónoma de Madrid, Madrid, Spain

J. Cuevas, J. Fernandez Menendez, S. Folgueras, I. Gonzalez Caballero, E. Palencia Cortezon, J.M. Vizan Garcia

Universidad de Oviedo, Oviedo, Spain

I.J. Cabrillo, A. Calderon, J.R. Castiñeiras De Saa, P. De Castro Manzano, J. Duarte Campderros, M. Fernandez, J. Garcia-Ferrero, G. Gomez, A. Lopez Virto, J. Marco, R. Marco, C. Martinez Rivero, F. Matorras, F.J. Munoz Sanchez, J. Piedra Gomez, T. Rodrigo, A.Y. Rodríguez-Marrero, A. Ruiz-Jimeno, L. Scodellaro, I. Vila, R. Vilar Cortabitarte

Instituto de Física de Cantabria (IFCA), CSIC-Universidad de Cantabria, Santander, Spain

D. Abbaneo, E. Auffray, G. Auzinger, M. Bachtis, P. Baillon, A.H. Ball, D. Barney, A. Benaglia, J. Bendavid, L. Benhabib, J.F. Benitez, G.M. Berruti, P. Bloch, A. Bocci, A. Bonato, C. Botta, H. Breuker, T. Camporesi, R. Castello, G. Cerminara, S. Colafranceschi [40], M. D'Alfonso, D. d'Enterria, A. Dabrowski, V. Daponte, A. David, M. De Gruttola, F. De Guio, A. De Roeck, S. De Visscher, E. Di Marco, M. Dobson, M. Dordevic, B. Dorney, T. du Pree, M. Dünser, N. Dupont, A. Elliott-Peisert, G. Franzoni, W. Funk, D. Gigi, K. Gill, D. Giordano, M. Girone, F. Glege, R. Guida, S. Gundacker, M. Guthoff, J. Hammer, P. Harris, J. Hegeman, V. Innocente, P. Janot, H. Kirschenmann, M.J. Kortelainen, K. Kousouris, K. Krajczar, P. Lecoq, C. Lourenço, M.T. Lucchini, N. Magini, L. Malgeri, M. Mannelli, A. Martelli, L. Masetti, F. Meijers, S. Mersi, E. Meschi, F. Moortgat, S. Morovic, M. Mulders, M.V. Nemallapudi, H. Neugebauer, S. Orfanelli [41], L. Orsini, L. Pape, E. Perez, M. Peruzzi, A. Petrilli, G. Petrucciani, A. Pfeiffer, D. Piparo, A. Racz, G. Rolandi [42], M. Rovere, M. Ruan, H. Sakulin, C. Schäfer, C. Schwick, A. Sharma, P. Silva, M. Simon, P. Sphicas [43], D. Spiga, J. Steggemann, B. Stieger, M. Stoye, Y. Takahashi, D. Treille, A. Triossi, A. Tsirou, G.I. Veres [20], N. Wardle, H.K. Wöhri, A. Zagozdzinska [34], W.D. Zeuner

CERN, European Organization for Nuclear Research, Geneva, Switzerland

W. Bertl, K. Deiters, W. Erdmann, R. Horisberger, Q. Ingram, H.C. Kaestli, D. Kotlinski, U. Langenegger, D. Renker, T. Rohe

Paul Scherrer Institut, Villigen, Switzerland

F. Bachmair, L. Bäni, L. Bianchini, M.A. Buchmann, B. Casal, G. Dissertori, M. Dittmar, M. Donegà, P. Eller, C. Grab, C. Heidegger, D. Hits, J. Hoss, G. Kasieczka, W. Lustermann, B. Mangano, M. Marionneau, P. Martinez Ruiz del Arbol, M. Masciovecchio, D. Meister, F. Micheli, P. Musella, F. Nessi-Tedaldi, F. Pandolfi, J. Pata, F. Pauss, L. Perrozzi, M. Quittnat, M. Rossini, A. Starodumov [44], M. Takahashi, V.R. Tavolaro, K. Theofilatos, R. Wallny

Institute for Particle Physics, ETH Zurich, Zurich, Switzerland

T.K. Aarrestad, C. Amsler [45], L. Caminada, M.F. Canelli, V. Chiochia, A. De Cosa, C. Galloni, A. Hinzmann, T. Hreus, B. Kilminster, C. Lange, J. Ngadiuba, D. Pinna, P. Robmann, F.J. Ronga, D. Salerno, Y. Yang

Universität Zürich, Zurich, Switzerland

M. Cardaci, K.H. Chen, T.H. Doan, Sh. Jain, R. Khurana, M. Konyushikhin, C.M. Kuo, W. Lin, Y.J. Lu, S.S. Yu

National Central University, Chung-Li, Taiwan

Arun Kumar, R. Bartek, P. Chang, Y.H. Chang, Y.W. Chang, Y. Chao, K.F. Chen, P.H. Chen, C. Dietz, F. Fiori, U. Grundler, W.-S. Hou, Y. Hsiung, Y.F. Liu, R.-S. Lu, M. Miñano Moya, E. Petrakou, J.f. Tsai, Y.M. Tzeng

National Taiwan University (NTU), Taipei, Taiwan

B. Asavapibhop, K. Kovitanggoon, G. Singh, N. Srimanobhas, N. Suwonjandee

Chulalongkorn University, Faculty of Science, Department of Physics, Bangkok, Thailand

A. Adiguzel, S. Cerci [46], Z.S. Demiroglu, C. Dozen, I. Dumanoglu, S. Girgis, G. Gokbulut, Y. Guler, E. Gurpinar, I. Hos, E.E. Kangal [47], A. Kayis Topaksu, G. Onengut [48], K. Ozdemir [49], S. Ozturk [50], B. Tali [46], H. Topakli [50], M. Vergili, C. Zorbilmez

Cukurova University, Adana, Turkey

I.V. Akin, B. Bilin, S. Bilmis, B. Isildak [51], G. Karapinar [52], M. Yalvac, M. Zeyrek

Middle East Technical University, Physics Department, Ankara, Turkey

E.A. Albayrak [53], E. Gülmez, M. Kaya [54], O. Kaya [55], T. Yetkin [56]

Bogazici University, Istanbul, Turkey

K. Cankocak, S. Sen [57], F.I. Vardarlı

Istanbul Technical University, Istanbul, Turkey

B. Grynyov

Institute for Scintillation Materials of National Academy of Science of Ukraine, Kharkov, Ukraine

L. Levchuk, P. Sorokin

National Scientific Center, Kharkov Institute of Physics and Technology, Kharkov, Ukraine

R. Aggleton, F. Ball, L. Beck, J.J. Brooke, E. Clement, D. Cussans, H. Flacher, J. Goldstein, M. Grimes, G.P. Heath, H.F. Heath, J. Jacob, L. Kreczko, C. Lucas, Z. Meng, D.M. Newbold [58], S. Paramesvaran, A. Poll, T. Sakuma, S. Seif El Nasr-storey, S. Senkin, D. Smith, V.J. Smith

University of Bristol, Bristol, United Kingdom

K.W. Bell, A. Belyaev [59], C. Brew, R.M. Brown, D. Cieri, D.J.A. Cockerill, J.A. Coughlan, K. Harder, S. Harper, E. Olaiya, D. Petyt, C.H. Shepherd-Themistocleous, A. Thea, I.R. Tomalin, T. Williams, W.J. Womersley, S.D. Worm

Rutherford Appleton Laboratory, Didcot, United Kingdom

M. Baber, R. Bainbridge, O. Buchmuller, A. Bundock, D. Burton, S. Casasso, M. Citron, D. Colling, L. Corpe, N. Cripps, P. Dauncey, G. Davies, A. De Wit, M. Della Negra, P. Dunne, A. Elwood, W. Ferguson, J. Fulcher, D. Futyan, G. Hall, G. Iles, M. Kenzie, R. Lane, R. Lucas [58], L. Lyons, A.-M. Magnan, S. Malik, J. Nash, A. Nikitenko [44], J. Pela, M. Pesaresi, K. Petridis, D.M. Raymond, A. Richards, A. Rose, C. Seez, A. Tapper, K. Uchida, M. Vazquez Acosta [60], T. Virdee, S.C. Zenz

Imperial College, London, United Kingdom

J.E. Cole, P.R. Hobson, A. Khan, P. Kyberd, D. Leggat, D. Leslie, I.D. Reid, P. Symonds, L. Teodorescu, M. Turner

Brunel University, Uxbridge, United Kingdom

A. Borzou, K. Call, J. Dittmann, K. Hatakeyama, A. Kasmi, H. Liu, N. Pastika

Baylor University, Waco, USA

O. Charaf, S.I. Cooper, C. Henderson, P. Rumerio

The University of Alabama, Tuscaloosa, USA

A. Avetisyan, T. Bose, C. Fantasia, D. Gastler, P. Lawson, D. Rankin, C. Richardson, J. Rohlf, J. St. John, L. Sulak, D. Zou

Boston University, Boston, USA

J. Alimena, E. Berry, S. Bhattacharya, D. Cutts, N. Dhingra, A. Ferapontov, A. Garabedian, J. Hakala, U. Heintz, E. Laird, G. Landsberg, Z. Mao, M. Narain, S. Piperov, S. Sagir, T. Sinthuprasith, R. Syarif

Brown University, Providence, USA

R. Breedon, G. Breto, M. Calderon De La Barca Sanchez, S. Chauhan, M. Chertok, J. Conway, R. Conway, P.T. Cox, R. Erbacher, M. Gardner, W. Ko, R. Lander, M. Mulhearn, D. Pellett, J. Pilot, F. Ricci-Tam, S. Shalhout, J. Smith, M. Squires, D. Stolp, M. Tripathi, S. Wilbur, R. Yohay

University of California, Davis, Davis, USA

R. Cousins, P. Everaerts, C. Farrell, J. Hauser, M. Ignatenko, D. Saltzberg, E. Takasugi, V. Valuev, M. Weber

University of California, Los Angeles, USA

K. Burt, R. Clare, J. Ellison, J.W. Gary, G. Hanson, J. Heilman, M. Ivova Paneva, P. Jandir, E. Kennedy, F. Lacroix, O.R. Long, A. Luthra, M. Malberti, M. Olmedo Negrete, A. Shrinivas, H. Wei, S. Wimpenny, B.R. Yates

University of California, Riverside, Riverside, USA

J.G. Branson, G.B. Cerati, S. Cittolin, R.T. D'Agnolo, A. Holzner, R. Kelley, D. Klein, J. Letts, I. Macneill, D. Olivito, S. Padhi, M. Pieri, M. Sani, V. Sharma, S. Simon, M. Tadel, A. Vartak, S. Wasserbaech [61], C. Welke, F. Würthwein, A. Yagil, G. Zevi Della Porta

University of California, San Diego, La Jolla, USA

D. Barge, J. Bradmiller-Feld, C. Campagnari, A. Dishaw, V. Dutta, K. Flowers, M. Franco Sevilla, P. Geffert, C. George, F. Golf, L. Gouskos, J. Gran, J. Incandela, C. Justus, N. Mccoll, S.D. Mullin, J. Richman, D. Stuart, I. Suarez, W. To, C. West, J. Yoo

University of California, Santa Barbara, Santa Barbara, USA

D. Anderson, A. Apresyan, A. Bornheim, J. Bunn, Y. Chen, J. Duarte, A. Mott, H.B. Newman, C. Pena, M. Pierini, M. Spiropulu, J.R. Vlimant, S. Xie, R.Y. Zhu

California Institute of Technology, Pasadena, USA

M.B. Andrews, V. Azzolini, A. Calamba, B. Carlson, T. Ferguson, M. Paulini, J. Russ, M. Sun, H. Vogel, I. Vorobiev

Carnegie Mellon University, Pittsburgh, USA

J.P. Cumalat, W.T. Ford, A. Gaz, F. Jensen, A. Johnson, M. Krohn, T. Mulholland, U. Nauenberg, K. Stenson, S.R. Wagner

University of Colorado Boulder, Boulder, USA

J. Alexander, A. Chatterjee, J. Chaves, J. Chu, S. Dittmer, N. Eggert, N. Mirman, G. Nicolas Kaufman, J.R. Patterson, A. Rinkevicius, A. Ryd, L. Skinnari, L. Soffi, W. Sun, S.M. Tan, W.D. Teo, J. Thom, J. Thompson, J. Tucker, Y. Weng, P. Wittich

Cornell University, Ithaca, USA

S. Abdullin, M. Albrow, J. Anderson, G. Apollinari, S. Banerjee, L.A.T. Bauerdick, A. Beretvas, J. Berryhill, P.C. Bhat, G. Bolla, K. Burkett, J.N. Butler, H.W.K. Cheung, F. Chlebana, S. Cihangir, V.D. Elvira, I. Fisk, J. Freeman, E. Gottschalk, L. Gray, D. Green, S. Grünendahl, O. Gutsche, J. Hanlon, D. Hare, R.M. Harris, J. Hirschauer, Z. Hu, S. Jindariani, M. Johnson, U. Joshi, A.W. Jung, B. Klima, B. Kreis, S. Kwan †, S. Lammel, J. Linacre, D. Lincoln, R. Lipton, T. Liu, R. Lopes De Sá, J. Lykken, K. Maeshima, J.M. Marraffino, V.I. Martinez Outschoorn, S. Maruyama, D. Mason, P. McBride, P. Merkel, K. Mishra, S. Mrenna, S. Nahn, C. Newman-Holmes, V. O'Dell, K. Pedro, O. Prokofyev, G. Rakness, E. Sexton-Kennedy, A. Soha, W.J. Spalding, L. Spiegel, L. Taylor, S. Tkaczyk, N.V. Tran, L. Uplegger, E.W. Vaandering, C. Vernieri, M. Verzocchi, R. Vidal, H.A. Weber, A. Whitbeck, F. Yang

Fermi National Accelerator Laboratory, Batavia, USA

D. Acosta, P. Avery, P. Bortignon, D. Bourilkov, A. Carnes, M. Carver, D. Curry, S. Das, G.P. Di Giovanni, R.D. Field, I.K. Furic, J. Hugon, J. Konigsberg, A. Korytov, J.F. Low, P. Ma, K. Matchev, H. Mei, P. Milenovic [62], G. Mitselmakher, D. Rank, R. Rossin, L. Shchutska, M. Snowball, D. Sperka, N. Terentyev, L. Thomas, J. Wang, S. Wang, J. Yelton

University of Florida, Gainesville, USA

S. Hewamanage, S. Linn, P. Markowitz, G. Martinez, J.L. Rodriguez

Florida International University, Miami, USA

A. Ackert, J.R. Adams, T. Adams, A. Askew, J. Bochenek, B. Diamond, J. Haas, S. Hagopian, V. Hagopian, K.F. Johnson, A. Khatiwada, H. Prosper, V. Veeraraghavan, M. Weinberg

Florida State University, Tallahassee, USA

M.M. Baarmand, V. Bhopatkar, M. Hohlmann, H. Kalakhety, D. Noonan, T. Roy, F. Yumiceva

Florida Institute of Technology, Melbourne, USA

M.R. Adams, L. Apanasevich, D. Berry, R.R. Betts, I. Bucinskaite, R. Cavanaugh, O. Evdokimov, L. Gauthier, C.E. Gerber, D.J. Hofman, P. Kurt, C. O'Brien, I.D. Sandoval Gonzalez, C. Silkworth, P. Turner, N. Varelas, Z. Wu, M. Zakaria

University of Illinois at Chicago (UIC), Chicago, USA

B. Bilki [63], W. Clarida, K. Dilsiz, S. Durgut, R.P. Gandrajula, M. Haytmyradov, V. Khristenko, J.-P. Merlo, H. Mermerkaya [64], A. Mestvirishvili, A. Moeller, J. Nachtman, H. Ogul, Y. Onel, F. Ozok [53], A. Penzo, C. Snyder, P. Tan, E. Tiras, J. Wetzel, K. Yi

The University of Iowa, Iowa City, USA

I. Anderson, B.A. Barnett, B. Blumenfeld, D. Fehling, L. Feng, A.V. Gritsan, P. Maksimovic, C. Martin, M. Osherson, M. Swartz, M. Xiao, Y. Xin, C. You

Johns Hopkins University, Baltimore, USA

P. Baringer, A. Bean, G. Benelli, C. Bruner, R.P. Kenny III, D. Majumder, M. Malek, M. Murray, S. Sanders, R. Stringer, Q. Wang

The University of Kansas, Lawrence, USA

A. Ivanov, K. Kaadze, S. Khalil, M. Makouski, Y. Maravin, A. Mohammadi, L.K. Saini, N. Skhirtladze, S. Toda

Kansas State University, Manhattan, USA

D. Lange, F. Rebassoo, D. Wright

Lawrence Livermore National Laboratory, Livermore, USA

C. Anelli, A. Baden, O. Baron, A. Belloni, B. Calvert, S.C. Eno, C. Ferraioli, J.A. Gomez, N.J. Hadley, S. Jabeen, R.G. Kellogg, T. Kolberg, J. Kunkle, Y. Lu, A.C. Mignerey, Y.H. Shin, A. Skuja, M.B. Tonjes, S.C. Tonwar

University of Maryland, College Park, USA

A. Apyan, R. Barbieri, A. Baty, K. Bierwagen, S. Brandt, W. Busza, I.A. Cali, Z. Demiragli, L. Di Matteo, G. Gomez Ceballos, M. Goncharov, D. Gulhan, Y. Iiyama, G.M. Innocenti, M. Klute, D. Kovalskyi, Y.S. Lai, Y.-J. Lee, A. Levin, P.D. Luckey, A.C. Marini, C. Mcginn, C. Mironov, X. Niu, C. Paus, D. Ralph, C. Roland, G. Roland, J. Salfeld-Nebgen, G.S.F. Stephans, K. Sumorok, M. Varma, D. Velicanu, J. Veverka, J. Wang, T.W. Wang, B. Wyslouch, M. Yang, V. Zhukova

Massachusetts Institute of Technology, Cambridge, USA

B. Dahmes, A. Evans, A. Finkel, A. Gude, P. Hansen, S. Kalafut, S.C. Kao, K. Klapoetke, Y. Kubota, Z. Lesko, J. Mans, S. Nourbakhsh, N. Ruckstuhl, R. Rusack, N. Tambe, J. Turkewitz

University of Minnesota, Minneapolis, USA

J.G. Acosta, S. Oliveros

University of Mississippi, Oxford, USA

E. Avdeeva, K. Bloom, S. Bose, D.R. Claes, A. Dominguez, C. Fangmeier, R. Gonzalez Suarez, R. Kamalieddin, J. Keller, D. Knowlton, I. Kravchenko, J. Lazo-Flores, F. Meier, J. Monroy, F. Ratnikov, J.E. Siado, G.R. Snow

University of Nebraska–Lincoln, Lincoln, USA

M. Alyari, J. Dolen, J. George, A. Godshalk, C. Harrington, I. Iashvili, J. Kaisen, A. Kharchilava, A. Kumar, S. Rappoccio

State University of New York at Buffalo, Buffalo, USA

G. Alverson, E. Barberis, D. Baumgartel, M. Chasco, A. Hortiangtham, A. Massironi, D.M. Morse, D. Nash, T. Orimoto, R. Teixeira De Lima, D. Trocino, R.-J. Wang, D. Wood, J. Zhang

Northeastern University, Boston, USA

K.A. Hahn, A. Kubik, N. Mucia, N. Odell, B. Pollack, A. Pozdnyakov, M. Schmitt, S. Stoynev, K. Sung, M. Trovato, M. Velasco

Northwestern University, Evanston, USA

A. Brinkerhoff, N. Dev, M. Hildreth, C. Jessop, D.J. Karmgard, N. Kellams, K. Lannon, S. Lynch, N. Marinelli, F. Meng, C. Mueller, Y. Musienko [35], T. Pearson, M. Planer, A. Reinsvold, R. Ruchti, G. Smith, S. Taroni, N. Valls, M. Wayne, M. Wolf, A. Woodard

University of Notre Dame, Notre Dame, USA

L. Antonelli, J. Brinson, B. Bylsma, L.S. Durkin, S. Flowers, A. Hart, C. Hill, R. Hughes, W. Ji, K. Kotov, T.Y. Ling, B. Liu, W. Luo, D. Puigh, M. Rodenburg, B.L. Winer, H.W. Wulsin

The Ohio State University, Columbus, USA

O. Driga, P. Elmer, J. Hardenbrook, P. Hebda, S.A. Koay, P. Lujan, D. Marlow, T. Medvedeva, M. Mooney, J. Olsen, C. Palmer, P. Piroué, X. Quan, H. Saka, D. Stickland, C. Tully, J.S. Werner, A. Zuranski

Princeton University, Princeton, USA

S. Malik

University of Puerto Rico, Mayaguez, USA

V.E. Barnes, D. Benedetti, D. Bortoletto, L. Gutay, M.K. Jha, M. Jones, K. Jung, M. Kress, D.H. Miller, N. Neumeister, B.C. Radburn-Smith, X. Shi, I. Shipsey, D. Silvers, J. Sun, A. Svyatkovskiy, F. Wang, W. Xie, L. Xu

Purdue University, West Lafayette, USA

N. Parashar, J. Stupak

Purdue University Calumet, Hammond, USA

A. Adair, B. Akgun, Z. Chen, K.M. Ecklund, F.J.M. Geurts, M. Guilbaud, W. Li, B. Michlin, M. Northup, B.P. Padley, R. Redjimi, J. Roberts, J. Rorie, Z. Tu, J. Zabel

Rice University, Houston, USA

B. Betchart, A. Bodek, P. de Barbaro, R. Demina, Y. Eshaq, T. Ferbel, M. Galanti, A. Garcia-Bellido, J. Han, A. Harel, O. Hindrichs, A. Khukhunaishvili, G. Petrillo, M. Verzetti

University of Rochester, Rochester, USA

L. Demortier

The Rockefeller University, New York, USA

S. Arora, A. Barker, J.P. Chou, C. Contreras-Campana, E. Contreras-Campana, D. Duggan, D. Ferencek, Y. Gershtein, R. Gray, E. Halkiadakis, D. Hidas, E. Hughes, S. Kaplan, R. Kunnawalkam Elayavalli, A. Lath, K. Nash, S. Panwalkar, M. Park, S. Salur, S. Schnetzer, D. Sheffield, S. Somalwar, R. Stone, S. Thomas, P. Thomassen, M. Walker

Rutgers, The State University of New Jersey, Piscataway, USA

M. Foerster, G. Riley, K. Rose, S. Spanier, A. York

University of Tennessee, Knoxville, USA

O. Bouhali [65], A. Castaneda Hernandez [65], M. Dalchenko, M. De Mattia, A. Delgado, S. Dildick, R. Eusebi, W. Flanagan, J. Gilmore, T. Kamon [66], V. Krutelyov, R. Mueller, I. Osipenkov, Y. Pakhotin, R. Patel, A. Perloff, A. Rose, A. Safonov, A. Tatarinov, K.A. Ulmer [2]

Texas A&M University, College Station, USA

N. Akchurin, C. Cowden, J. Damgov, C. Dragoiu, P.R. Dudero, J. Faulkner, S. Kunori, K. Lamichhane, S.W. Lee, T. Libeiro, S. Undleeb, I. Volobouev

Texas Tech University, Lubbock, USA

E. Appelt, A.G. Delannoy, S. Greene, A. Gurrola, R. Janjam, W. Johns, C. Maguire, Y. Mao, A. Melo, H. Ni, P. Sheldon, B. Snook, S. Tuo, J. Velkovska, Q. Xu

Vanderbilt University, Nashville, USA

M.W. Arenton, S. Boutle, B. Cox, B. Francis, J. Goodell, R. Hirosky, A. Ledovskoy, H. Li, C. Lin, C. Neu, X. Sun, Y. Wang, E. Wolfe, J. Wood, F. Xia

University of Virginia, Charlottesville, USA

C. Clarke, R. Harr, P.E. Karchin, C. Kottachchi Kankanamge Don, P. Lamichhane, J. Sturdy

Wayne State University, Detroit, USA

D.A. Belknap, D. Carlsmith, M. Cepeda, A. Christian, S. Dasu, L. Dodd, S. Duric, E. Friis, B. Gomber, M. Grothe, R. Hall-Wilton, M. Herndon, A. Hervé, P. Klabbers, A. Lanaro, A. Levine, K. Long, R. Loveless, A. Mohapatra, I. Ojalvo, T. Perry, G.A. Pierro, G. Polese, T. Ruggles, T. Sarangi, A. Savin, A. Sharma, N. Smith, W.H. Smith, D. Taylor, N. Woods

University of Wisconsin–Madison, Madison, WI, USA

† Deceased.
[1] Also at Vienna University of Technology, Vienna, Austria.
[2] Also at CERN, European Organization for Nuclear Research, Geneva, Switzerland.
[3] Also at State Key Laboratory of Nuclear Physics and Technology, Peking University, Beijing, China.
[4] Also at Institut Pluridisciplinaire Hubert Curien, Université de Strasbourg, Université de Haute Alsace Mulhouse, CNRS/IN2P3, Strasbourg, France.
[5] Also at National Institute of Chemical Physics and Biophysics, Tallinn, Estonia.
[6] Also at Skobeltsyn Institute of Nuclear Physics, Lomonosov Moscow State University, Moscow, Russia.
[7] Also at Universidade Estadual de Campinas, Campinas, Brazil.
[8] Also at Centre National de la Recherche Scientifique (CNRS) - IN2P3, Paris, France.
[9] Also at Laboratoire Leprince-Ringuet, Ecole Polytechnique, IN2P3-CNRS, Palaiseau, France.
[10] Also at Joint Institute for Nuclear Research, Dubna, Russia.
[11] Also at Beni-Suef University, Bani Sweif, Egypt.
[12] Now at British University in Egypt, Cairo, Egypt.
[13] Also at Ain Shams University, Cairo, Egypt.
[14] Also at Zewail City of Science and Technology, Zewail, Egypt.
[15] Also at Université de Haute Alsace, Mulhouse, France.
[16] Also at Tbilisi State University, Tbilisi, Georgia.
[17] Also at University of Hamburg, Hamburg, Germany.
[18] Also at Brandenburg University of Technology, Cottbus, Germany.
[19] Also at Institute of Nuclear Research ATOMKI, Debrecen, Hungary.
[20] Also at Eötvös Loránd University, Budapest, Hungary.
[21] Also at University of Debrecen, Debrecen, Hungary.
[22] Also at Wigner Research Centre for Physics, Budapest, Hungary.
[23] Also at University of Visva-Bharati, Santiniketan, India.
[24] Now at King Abdulaziz University, Jeddah, Saudi Arabia.
[25] Also at University of Ruhuna, Matara, Sri Lanka.
[26] Also at Isfahan University of Technology, Isfahan, Iran.
[27] Also at University of Tehran, Department of Engineering Science, Tehran, Iran.
[28] Also at Plasma Physics Research Center, Science and Research Branch, Islamic Azad University, Tehran, Iran.
[29] Also at Università degli Studi di Siena, Siena, Italy.
[30] Also at Purdue University, West Lafayette, USA.
[31] Also at International Islamic University of Malaysia, Kuala Lumpur, Malaysia.
[32] Also at Malaysian Nuclear Agency, MOSTI, Kajang, Malaysia.
[33] Also at Consejo Nacional de Ciencia y Tecnología, Mexico city, Mexico.
[34] Also at Warsaw University of Technology, Institute of Electronic Systems, Warsaw, Poland.
[35] Also at Institute for Nuclear Research, Moscow, Russia.
[36] Also at St. Petersburg State Polytechnical University, St. Petersburg, Russia.
[37] Also at National Research Nuclear University 'Moscow Engineering Physics Institute' (MEPhI), Moscow, Russia.
[38] Also at California Institute of Technology, Pasadena, USA.

[39] Also at Faculty of Physics, University of Belgrade, Belgrade, Serbia.
[40] Also at Facoltà Ingegneria, Università di Roma, Roma, Italy.
[41] Also at National Technical University of Athens, Athens, Greece.
[42] Also at Scuola Normale e Sezione dell'INFN, Pisa, Italy.
[43] Also at University of Athens, Athens, Greece.
[44] Also at Institute for Theoretical and Experimental Physics, Moscow, Russia.
[45] Also at Albert Einstein Center for Fundamental Physics, Bern, Switzerland.
[46] Also at Adiyaman University, Adiyaman, Turkey.
[47] Also at Mersin University, Mersin, Turkey.
[48] Also at Cag University, Mersin, Turkey.
[49] Also at Piri Reis University, Istanbul, Turkey.
[50] Also at Gaziosmanpasa University, Tokat, Turkey.
[51] Also at Ozyegin University, Istanbul, Turkey.
[52] Also at Izmir Institute of Technology, Izmir, Turkey.
[53] Also at Mimar Sinan University, Istanbul, Istanbul, Turkey.
[54] Also at Marmara University, Istanbul, Turkey.
[55] Also at Kafkas University, Kars, Turkey.
[56] Also at Yildiz Technical University, Istanbul, Turkey.
[57] Also at Hacettepe University, Ankara, Turkey.
[58] Also at Rutherford Appleton Laboratory, Didcot, United Kingdom.
[59] Also at School of Physics and Astronomy, University of Southampton, Southampton, United Kingdom.
[60] Also at Instituto de Astrofísica de Canarias, La Laguna, Spain.
[61] Also at Utah Valley University, Orem, USA.
[62] Also at University of Belgrade, Faculty of Physics and Vinca Institute of Nuclear Sciences, Belgrade, Serbia.
[63] Also at Argonne National Laboratory, Argonne, USA.
[64] Also at Erzincan University, Erzincan, Turkey.
[65] Also at Texas A&M University at Qatar, Doha, Qatar.
[66] Also at Kyungpook National University, Daegu, Korea.